Progress in TiO2 nanotube coatings for biomedical applications : a review

Cheng, Yan; Yang, Hui; Yang, Yun; Huang, Jianying; Wu, Ke; Chen, Zhong; Wang, Xiaoqin; Lin, Changjian; Lai, Yuekun

2018

Cheng, Y., Yang, H., Yang, Y., Huang, J., Wu, K., Chen, Z., . .. Lai, Y. (2018). Progress in TiO2 nanotube coatings for biomedical applications : a review. Journal of Materials Chemistry B, 6(13), 1862-1886. doi:10.1039/C8TB00149A

https://hdl.handle.net/10356/85995

https://doi.org/10.1039/C8TB00149A

Progress in TiO_2 nanotube coatings for biomedical applications: A review

Received 00th January 20xx,
Accepted 00th January 20xx

DOI: 10.1039/x0xx00000x

www.rsc.org/

Yan Cheng,[a†] Hui Yang,[a†] Yun Yang,[b†] Jianying Huang,[a] Zhong Chen,[c] Xiaoqing Wang,[a] Changjian Lin[b] and Yuekun Lai[*,a]

Abstract: Titanium dioxide nanotubes (TNTs) have drawn wide attention and been extensively applied in the field of biomedicine, due to their large specific surface area, good corrosion resistance, excellent biocompatibility and enhanced bioactivity. This review describes the preparation of TNTs and the surface modification which entrust the nanotubes with better antibacterial property and enhanced osteoblast adhesion, proliferation and differentiation. Considering the contact between TNTs surface and surrounding tissues after implantation, the interactions between TNTs (with properties including diameter, length, wettability and crystalline phase) and proteins, platelets, bacteria and cells are illustrated. The state of the art in the applications of TNTs in dentistry, orthopedic implants and cardiovascular stents have been introduced. In particular, the application of TNTs in biosensing has attracted much attention due to its ability of rapid diagnosis of diseases. Finally, the difficulties and challenges for practical application of TNTs are also discussed.

1. Introduction

Titanium dioxide (TiO_2) has been widely used as pigment, paints, ointments and toothpaste,[1-3] and has gained much more attention since photocatalytic water splitting was discovered on a TiO_2 electrode under ultraviolet (UV) light in 1972.[4] Then TiO_2 materials have been found a widely utilities range from energy to environmental applications, such as photocatalytic splitting, photoelectrodes, supercapacitors, dye-sensitized solar cells.[5-7]

Development in nanotechnology investigation has aroused production of different forms of TiO_2 nanostructures including nanotubes, nanowires, nanorods, nanobelts, and nanoribbons, which possess large surface area and high biocompatibility. These special TiO_2 nanostructures have attracted much interest in the biomedical field due to their unique and characteristic compatibility with the biological system, and their ability to integrate functional moieties on the surface which can modulate biological responses. In detail, taking advantages of the nanostructured hierarchy of biological structures when used in human body, synthetic nanostructured materials could replenish, stimulate and sustain physiological responses with little negative effects, for example promoting adsorption of extracellular proteins such as fibronectin and vitronectin. All these provide an advantageous environment for early cell adhesion on material surface. The nano-topography and nano-scale roughness of TNTs are in the similar size scale with the extracellular matrix signal particles, thus TNTs surface can provide topographic signals for cell recognition, regulate the expression of cellular signal molecules, and further improve the healthy tissue biomaterial integration. A series of experiments have demonstrated that TiO_2 nanostructures are attractive material for implant devices.

Implants, which were used to support, replace or augment a diseased or injured biological tissue, commonly applied as artificial hearts, prosthetic blood vessels, vascular stents, bone and dental structures. Metals, ceramics and polymers are the three main materials for implants. Metal implants with superior strength, stiffness and toughness are suitable for load-bearing applications.[8] Conversely, ceramics (including bioglass) have lower fracture toughness and higher elastic modulus than bone, so could not meet the demands of mechanical property *in vivo*.[9] Lastly, although polymer implants permit easy fixation to the surrounding tissue, polymers may evoke inflammation of the tissue if monomers leach out of the implants.[10, 11] In recent decades, TiO_2 nanotubes (TNTs) have drawn special attentions due to their high biocompatibility, osteoconduction and osseointegration. Howerer, the applications of TNTs still face big challenges due to the poor performance of antibacterial property and bioactivity.[12-14]

So far, a large amount of researches have been focused on the wide applications of TNTs in biomedical fields, especially various surface modified TNTs. Metallic nanoparticles (NPs) or drugs were loaded into TNTs to decrease post-operative infection. Hydroxyapatite (HA) was modified on TNTs surface to promote the integration of implants to bone tissue. Combinations of these strategies have also been reported to improve the bacterial resistance, osteogenesis and rate of osseointegration. In this review, recent research activities on the surface functionalization and biomedical applications of TNTs are illustrated. The synthesis methods and properties of TNTs, the interactions between TNTs and biomolecules and the surface functionalization of nanotubes were represented in details. Furthermore, the surface and interface interactions between TNTs and proteins, platelets, bacteria and cells are described to understand the effects of the diameter, length, crystalline phase and wettability of TNTs on cells and tissues. Finally, a comprehensive summary of biomedical TNTs materials are proposed, including their applications in dental and bone implants, vascular stents, biosensor and brain tumors.

2. Synthesis of TiO_2 nanotubes

TNTs can be fabricated by various synthesis techniques, such as template assisted, electrochemical anodization, hydrothermal and some other attractive approaches.[15]

2.1 Template assisted method

Template assisted method is an extremely popular synthesis method

[a] National Engineering Laboratory for Modern Silk, College of Textile and Clothing Engineering, Soochow University, Suzhou 215123, P. R. China.
[b] State Key Laboratory of Physical Chemistry of Solid Surfaces, Xiamen University, Xiamen 361005, P.R. China.
[c] School of Materials Science and Engineering, Nanyang Technological University, 50 Nanyang Avenue, Singapore.
[†] These authors contributed equally.
Corresponding Authors E-mail: yklai@suda.edu.cn

that prepares nanostructure with a morphology followed the known and characterized templates. In general, anodic aluminium oxide (AAO) and ZnO were most common used as the templates,[16, 17] because they can be selectively dissolved by chemical etching or solvent dissolution, leaving the resultants with a pre-set porosity and reversely duplicated morphology. Template assisted method can be divided into positive template and negative template.[18] With a positive method, the TiO_2 material is deposited outside of the template while negative template is deposited inside of the template structure.[19]

AAO was firstly used as the initial template to reproduce polymethyl methacrylate (PMMA) mould, and then amorphous TiO_2 was deposited onto the mould. The TNTs structure was successful achieved after dissolution of the polymer mould. The prepared nanotubes possessed a length of 8 mm, inner diameter about 70-100 nm and outer diameter around 140-180 nm.[20] Yuan *et al.* developed a template-directed synthesis apparatus, Where an AAO membrane was placed between two hales of a glass U-tube cell. As shown in Fig. 1A, two kinds of solutions in either half of the U-tube are allowed to diffuse across the holes of the AAO membrane and then react through hydrolysis or precipitation at the interface. Especially, the wall thickness of the TNTs can be tuned by carefully controlling the molar concentrations of $Ti(OC_4H_9)_4$.[21]

However, there are still some undeniable drawbacks about the template method. Firstly, the process of dissolving template not only generates waste and adds to the cost of material processing, but also have the risk of destroying the formed TiO_2 nanostructures. Moreover, the size of obtained TNTs is limited by the pore size of the template. Therefore, template methods are not suitable for the large scale preparation of TNTs.

2.2 Electrochemical anodization of TNTs

Electrochemical anodization is a versatile and cost-effective technique to produce TNTs with well-controlled structure and alignment.[22] Fig. 1B shows the apparatus for the electrochemical anodization. It comprises of an anode, which can be Ti or a Ti-based alloy, a cathode, which is usually platinum (Pt), and an electrolyte solution typically containing fluoride ion such as HF/NH_4F solution. The properties of TNTs could be easily controlled by anodization potential, electrolyte composition and concentration.

Anodized TiO_2 was first reported in 1984, and titanium metal was treated with alkaline peroxide etching and chromic acid anodization in turn.[23] In 2001, Gong *et al.* reported the preparation of well-aligned TNTs by titanium anodization in an aqueous solution containing 0.5 to 3.5 wt % hydrofluoric acid.[24] The prepared nanotube has a controllable diameter ranging from 25 to 65 nm (the value of diameter increased with applied voltage) but with a limited length of several hundred nanometers.

Lai *et al.* illustrated that the diameter of nanotube could be controlled by the anodization voltage, and the length of nanotube could be correlated with the anodic charge in Na_2SO_4/NaF electrolytes.[25] Highly-ordered TNTs arrays could also be prepared by potential anodization in fluoride ion containing non-aqueous organic polar electrolytes.[26]

Based on previous works, TNTs with large pore size were prepared successfully in a diethylene glycol electrolyte containing HF, and the anodization duration showed a more significant effect on pore diameter than the anodization voltage.[27] Yu *et al.* introduced a compact 200 nm thick oxide layer by employing an additional anodization in a fluoride-free electrolyte, which has led to a three-fold increase in the adhesion strength.[28] In conclusion, the structure of TNTs could be adjusted by electrolyte composition, pH, anodizing potential and temperature.[29]

2.3 Hydrothermal Treatment

Hydrothermal method is a simple and mature technique to synthesize TNTs.[30-32] At present, most accepted mechanism of hydrothermal for tube formation is that the TiO_2 NPs could turn into an intermediate state of exfoliated nanosheets under the hydrothermal reaction in NaOH solution. Then the nanosheets are spirally curled to nanotubes at a typical hydrothermal temperature range of 110-150 ℃. Through subsequent washing with dilute acidic aqueous solution or solvents such as water, a close to 100% yield of nanotubular products can be achieved.[33] Although the entire synthesis process seems to be very simple, each single step includes the choice of TiO_2 precursors, the hydrothermal condition (temperature, the concentration of reactants, and hydrothermal duration), and the subsequent post-synthesis washing procedure (washing times, acid concentration, and the sequence of washing by solvent and acid). All these play a crucial role in controlling the structure (crystallography and morphology) and physical-chemical properties of the final TNTs.

Other reported TNT formation mechanisms include the formation during acid washing, peeling-scrolling and seed-formation-oriented crystal growth. The Ti-O-Ti chemical bond in the TiO_2 nanoparticle could be destroyed by the NaOH solution in the hydrothermal reaction, and then ion-exchange occurs between Ti^+ and Na^+ which generates new chemical bonds (Ti-Na-O).[34] As shown in Fig. 1C, the process of pickling could promote the curling and folding of the nanosheet. The acid washing after the hydrothermal reaction could remove the Na^+ in the sample to reform the Ti-O-Ti bonds. The acid treatment could eliminate the electrostatic repulsion in the nanotube.[30] Liu and Zhang *et al.* fabricated nanotubes with the outer diameter of 50-80 nm and the wall thickness of 10 nm by gas-phase hydrothermal method, and observed the process of curling of nanosheets into tubes, which confirmed the curling mechanism.[35] Kukovecz *et al.* proposed a "crystal orientation growth" model to explain the possible mechanism of nanotubes forming, which is different from the previous models of film crimping and flaking.[36] The surface of TiO_2 grains will be covered with curly nanoloops while reacting with NaOH, and they believe that curvature of the nanoloops plays a key role in the nanotube structure.

The crystal structure and thermal stability of TNTs prepared by hydrothermal reaction are influenced by the crystal form, reaction temperature, reaction time and post-processing treatment. Different experimental parameters were studied to further reveal the key influence of the synthesis of TNTs. Poudel *et al.* suggested that the filling of the hydrothermal reactor greatly affected the final crystallinty of TNTs.[37] TNTs with different structures and properties are prepared with different reactants. TNTs with the outer diameter of 10-20 nm could be prepared with larger particle size of reactants (such as rutile, P25, hybrid SiO_2-TiO_2).[38] Temperature is also one of the important factors, and TNTs could be prepared with TiO_2 powders (anatase or rutile phase) and commercial P25 at hydrothermal

temperatures between 100 and 180 °C. When the temperature is out of this range, the amount of formed nanotubes will decrease.[39] Wang proposed that the morphology and size of nanostructures are primarily determined by the hydrothermal reaction rather than by the washing process, but also acknowledge that washing has some effect on the final nanostructures.[38] TNTs can also be formed during pickling after the hydrothermal reaction or in the washing process. As the last step, drying process could manage the morphology of nanotubes. Poudel *et al.* prepared TNTs by hydrothermal reaction, and TNTs were washed with deionized water and dried in an oven at 110 °C. The prepared TNTs have a length of 600 nm, an outer diameter of 9 nm and a wall thickness of 2.5 nm.

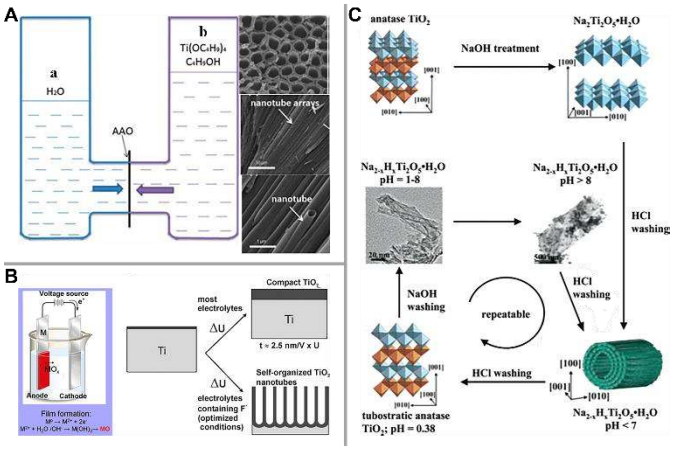

Fig. 1 Three different methods for the synthesis of TNTs: (A) Template assisted method. Adapted with permission from ref. 21. Copyright 2013 Royal society of chemistry. (B) Electrochemical anodization. Adapted with permission from ref. 22. Copyright 2014 Royal society of chemistry. (C) Thermal treatment. Adapted with permission from ref. 34. Copyright 2006 American Chemical Society.

3. Properties

3.1 Physicochemical properties

TiO_2 has four major crystal forms: the stable rutile (tetragonal, a = b = 4.584 Å, c = 2.953 Å), metastable anatase (tetragonal, a = b = 3.782 Å, c = 9.502 Å), brookite (rhombohedral, a = 5.436 Å, b = 9.166 Å, c = 5.135 Å) and TiO_2 (B) (monoclinic, a = 12.16 Å, b = 3.74 Å, c = 6.51 Å).[40-43] The basic structure of the TiO_2 crystal is titanyl octahedra (TiO_6). TiO_2 (B) was firstly prepared by Banfield through ion exchange and thermal treatment of $K_2Ti_4O_9$ in 1980,[44] which exhibited good thermal stability and could be converted to anatase at 800 °C. Brookite TiO_2 in powder or thin film form showing good stability and better (than anatase TiO_2) photocatalytic activity.[45] As shown in Fig. 2A, the octahedral of rutile phase (left) is irregular tending to rhombohedral, while anatase phase (right) showed obvious distortion of orthorhombic and the symmetry is lower than the former. Many factors such as crystallographic phases, particle size, surface area and surface hydroxyl have significant influences on the performance of titanium dioxide,[31, 46] and the transition from anatase to rutile is irreversible. The amorphous TNTs could be converted to anatase phase after annealing at 450 °C，then to a mixture of rutile and anatase after annealing at 550 °C, and the nanotubes lost their tubular structure at 650 °C.

At the same time, TiO_2 has strong photocatalytic activity under light irradiation, especially under UV irradiation.[47] The electron-hole description based on semiconductor energy band theory is a mature theory for the photocatalytic mechanism of TiO_2. As depicted in Fig. 2B, the electron in the valence band absorbs energy of photon and transits to the conduction band when irradiated by light with a wavelength shorter than the corresponding energy required for the electron transition. In the meantime, positively charged holes are left in the valence band. Electrons and holes could move freely and the movement of the charges can create a current as in any semiconductor materials. When the electrons/holes migrate to the surface of the TiO_2 particles, they may contact and react with air, water in the environment to generate hydroxyl and perhydroxyl radicals. These radicals have strong reactivity with a lot of ions and organics on the TiO_2 particles. The holes can react with surface-adsorbed H_2O to generate hydroxyl radicals. At the same time, the electrons are usually scavenged by O_2 to produce superoxide anion radicals. These substances in solution can react to give other cytotoxic reactive oxygen species (ROS) that are detrimental to cancer cells, such as hydrogen peroxide and peroxy radicals. The band gap of anatase is 3.2 eV and the rutile band gap is 3.0 eV. The higher band gap of anatase makes its electron-hole pairs have a more positive or negative potential and therefore has higher oxidation capacity.

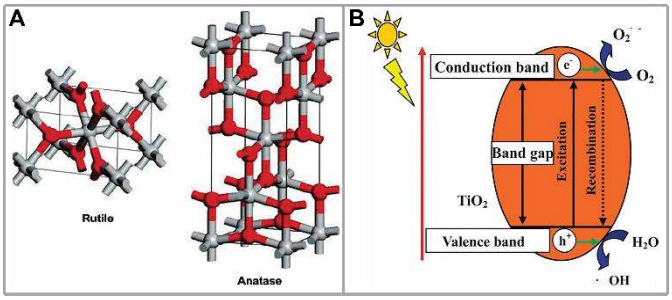

Fig. 2 (A) Bulk crystal structure of rutile (left) and anatase (right). (B) Titanium atoms are gray, and oxygen atoms are red and main processes in a photocatalytic reaction. Adapted with permission from ref. 47. Copyright 2006 American Chemical Society.

3.2 Bioactivity, biocompatibility and corrosion resistance

TiO_2 is extensively applied in biomedicine industry because of its good biocompatibility and corrosion resistance.[48-50] Biocompatibility is a central issue in current regenerative medicine and tissue engineering where the surface of implant materials is the key to "embedding" host organisms. TNTs possess good biocompatibility and become an advantageous platform for the growth and differentiation of osteoblasts. By controlling the morphology of nanotubes, it could be possible to enhance the activity of osteoblasts.[51, 52] Furthermore, titanium and titanium alloy biomaterials are considered to be corrosion resistant, because of a TiO_2 passivation layer, which is not readily soluble even in acidic media, formed on the surface. Therefore TiO_2 is often used as a corrosion resistant coating,[53] but the use of fluoride-containing dental formulations can alter the behavior of titanium in dentistry.[54]

Bioactive biomaterials can be divided into two categories: osteoconductive and osteoproductive. The former can be tied to hard tissue, such as tricalcium phosphate; and the other one can spontaneously bind itself to bone tissue and stimulate the growth of new bone on their surface, for example Ti and niobium.[55] Complex hydroxyapatite and biological macromolecules have been studied that combined with nanotubes to enhance the bioactivity.

4. Surface and interface interactions

4.1 Proteins interactions with TNTs

When implanted in the body, large amount of proteins will be adsorbed on the implant surface immediately. The adsorbed protein coating can serve as a mediator layer between the nanotube surface and cell membrane.[56] It has been found that proteins are prone to adsorb onto the TNTs instead of Ti, due to the high surface roughness of the TNTs (offering more sites for protein adsorption). Similarly, the cell adhesion is also selective with more cells favoring the TiO_2 nanotube surface, which can be attributed to selective protein adsorption.[57] Actually, proteins adsorption on the surface of nanostructured titanium consists of two steps. The first step is direct adhesion of molecules arriving at the surface, and the second process, which happened slower than the first process, is the rearrangement of molecular. Several parameters of the implanted biomaterials, such as surface charge density or electric field strength, topography and protein charge, could further influence the protein adsorption.

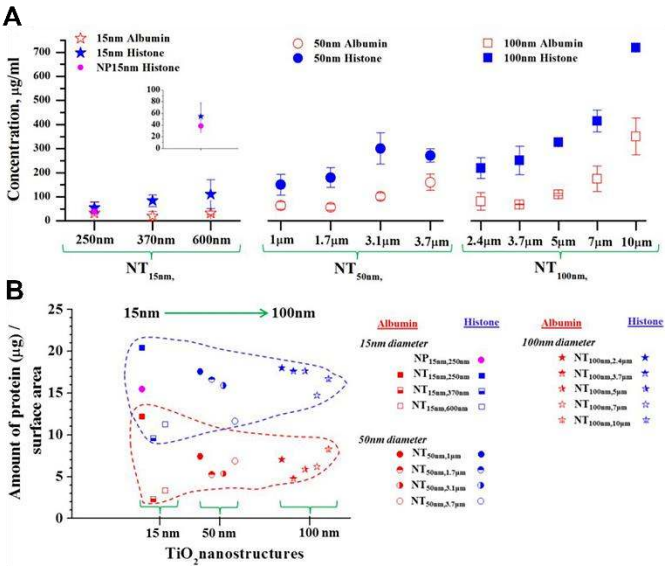

Fig. 3 (A) Concentration of protein adhesion (albumin, histone) on TiO_2 nanostructures as obtained from ELISA measurements; (B) Amount of adsorbed protein normalized with the dye desorption values. Adapted with permission from ref. 38. Copyright 2015 Dove Medical Press.

Kulkarni *et al.* further investigated the interactions between TNTs with different morphology and proteins, such as small sized bovine serum albumin (negatively charged) and histone (positively charged).[58] The result of enzyme-linked imminosorbent assay (ELISA) test is shown in the Fig. 3A. The highest adsorption of proteins occurred in the TNTs with diameter of 100 nm and length of 10 μm. The charge of the proteins is crucial, as titanium surface has a negative charge at a physiological pH, it is reasonable that the positive histone protein shows double amounts of adsorption compared with negative albumin.[59] In addition, TNTs with longer length were also beneficial to the protein adsorption, irrespective of protein charge. As shown in Fig. 3B, TNTs with increasing length, which amounts to increasing surface areas, leads to a small decrease in the adsorbed histone. As to albumin, the adsorbed amount is further limited by its charge.

Iglic *et al.* found that surface charge density and electric field strength could be locally increased by the surface nanostructure, due to highly curved nanoscale edges or protrusions, which further improved the adsorption of fibronectin.[60]

4.2 Platelets interaction with TNTs

The interaction between blood and implants has a significant influence on peri-implant healing.[61] Platelets, which adhere on the surface of implants quickly, play an important role in blood clotting, angiogenesis, and osteogenesis surrounding the implants.[62]

The exposure of implantable titanium and its alloys in the blood would lead to immunological action in the form of inflammation, thrombosis, fibrosis and infection, which causes implant failure. Nanoscale biomimetic architectures provide possible solutions for promoting hemocompatibility of titanium and its alloys. Smith *et al.* demonstrated that TNTs possess excellent blood-compatibility, and indicated this nanostructure can be used as a potential surface modification for blood-contacting implants. More research is needed into the relationship between nanotube diameter and the immune response.[63]

Some studies demonstrated that hemocompatibility can be altered by adjusting the diameter of TNTs. Further studies are focused on evaluating and understanding the effect of nanotube size and its specific components on hemocompatibility and immune response.[64]

Platelets adhesion on TNTs was also influenced by the different crystalline phases.[65] Research shows that TNTs annealed at 450 ℃ had the highest platelets adhesion value, followed by TNTs annealed at 350 ℃ and 550 ℃, and the amorphous Ti had the lowest adhesion value. The platelet on TNTs annealed at 450 °C exhibited a strong spreading trend and activating effect, thus TNTs with anatase phase have an obvious positive effect on platelets adhesion and activation.

Huang *et al.* studied the effects of TNT diameter and crystalline phases on platelets adhesion and activation.[66] As Fig 4A shows, highly organized, vertically aligned TNTs with various outer diameter and different annealing temperature were formed on the surface of titanium. The TNT structure completely collapsed leaving dense grains with irregular shapes after 800 ℃ annealing. Fig. 4B shows that large outer diameters led to the inhibition of platelet adhesion and activation, while small outer diameters with a predominately rutile phase had the same effect. Furthermore, fibrin network was found on TNTs with larger outer diameter and a predominately anatase phase. Thus, the interactions between platelets and TNTs were decided by a combination of nanotube size, crystalline phase and surface chemistry. This finding is helpful for the future design of TiO_2 based biomaterials. Besides diameter and crystalline phase, the surface wettability of TNTs is also one of the most critical factors on platelets adhesion.

Yang et al. prepared superhydrophilic and superhydrophobic TNTs layers by UV irradiation and surface modified with hydrophobic monolayer, respectively. The result of blood compatibility assay *in vitro* showed that superhydrophobic TNTs exhibited excellent blood compatibility and remarkable anti-adhesion of plateletse.[67] However, contradicting findings have been reported regarding the complicated needed.

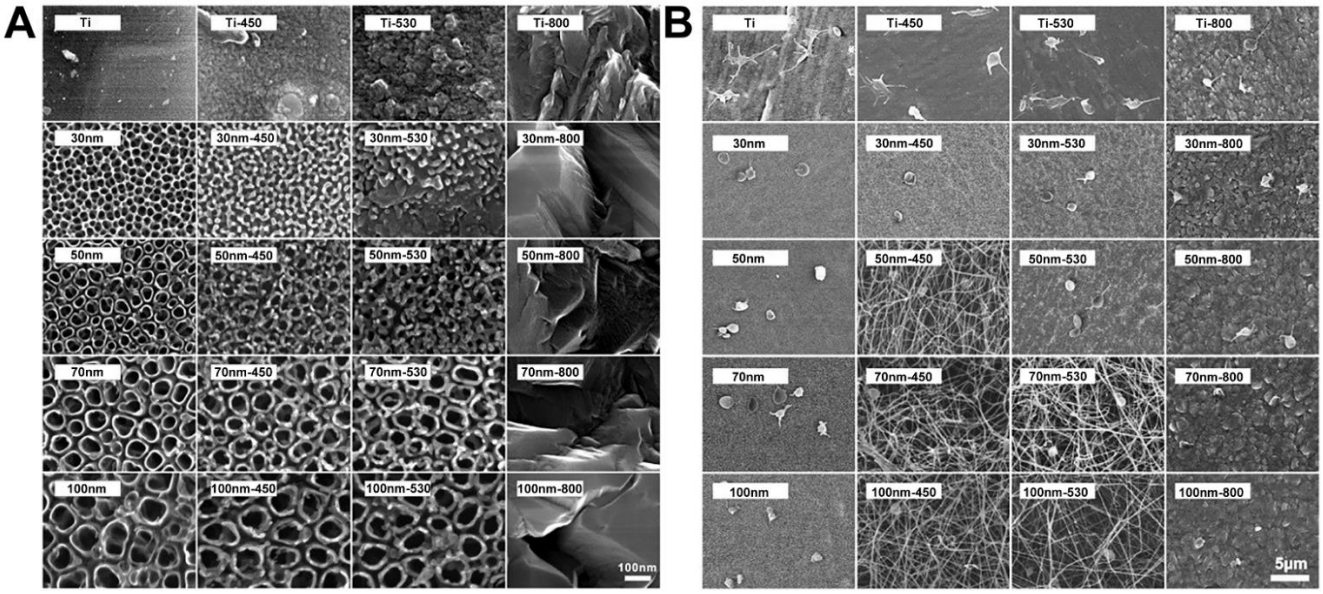

Fig. 4 (A) SEM images (top view) of titanium and self-aligned TNTs with different outer diameters (first column). The second to fourth columns present the corresponding samples annealed at 450 ℃ (second column), 530 ℃ (third column) and 800 ℃ (fourth column). (B) SEM morphology of adherent platelets on different samples. Adapted with permission from ref. 66. Copyright 2017 Elsevier.

4.3 Bacteria interaction with TNTs

Bacterial infection of medical implant is an increasingly serious issue that cannot be treated effectively by traditional antibiotics due to the growing prevalence of antimicrobial resistance.[68]

Previous studies demonstrated that nanometer sized Ti surface may be more useful for reducing the adhesion and activity of bacteria than untreated Ti.[69-72] Ercan *et al.* reported that bacterial adhesion can be adjusted by the physicochemical properties of TNTs such as surface chemistry, diameter and crystalline phase.[73] Specifically, the heat treatment could significantly decreased the amount of dead *Staphylococcus aureus* (*S. aureus*) and *Staphylococcus epidermidis* (*S. epidermidis*) bacteria adhering to the Ti surface, while larger Ti nanotubes decreased the amount of live bacteria compared to untreated Ti surface. Then the combined effect of heat treatment and diameter on bacteria adhesion were investigated. The result showed the 80 nm nanotube diameter possess the best antibacterial effect among all the treatment parameters. In addition, the fluorine content increased after anodized in HF electrolyte, the bacterial adhesion subsequently increased. The process of annealing nanotubes can remove some fluorine, which directly affected the bacteria adhesion and activity. Similarly, the adhesion of oral strepto-cocci on TNTs could also be controlled by nanotube diameter and fluoride content.[74] In addition, UV light and ethanol sterilization also decreased bacteria growth while autoclaving resulted in the highest amount of bacteria growth.[75]

The antibacterial activities of TNTs with different crystalline phases were also evaluated. TNTs with anatase phase showed best antibacterial activity among anatase, rutile and amorphous crystal phases. What is more, TNTs with 200 nm and 50 nm diameters also had much higher antibacterial activity than those with other diameters.[76] The antibacterial activity of the nanotubes was found to be independent on their lengths. In addition, it also found that the superhydrophobic modification has a double effects to inhibit bacterial adhesion and surface antibacterial ability.[77]

4.4 Cells interaction with TNTs

The interaction between cells and biomaterial surfaces is crucial for perfect clinical implants. In particular, many studies investigated the interaction between TNTs and various kinds of cells such as osteoblasts, fibroblasts, chondrocytes, endothelial cells, muscle cells, epidermal, keratinocytes and mesenchymal stem cell (MSC).[78] The effects of TNTs on cell adhesion, proliferation and differentiation depend on several factors, including diameter, crystalline phases, surface wettability, surface charge and chemical components.[79]

4.4.1 Diameter of TNTs

The surface morphology and roughness in nanoscale can serve as a signal of morphological effect, which provide favorable condition for cell adhesion and growth.[80] The vertically TNTs were reported to have a crucial effect on cell behavior such as adhesion, elongation, proliferation and related gene expression.[81-84] The nanotube size has a bigger impact than crystal form on the cell behavior.[85]

In the absence of specific pro-differentiation factors, TNTs with small diameter (about 30 nm) could promote cell adhesion, and those with diameter of 70-100 nm could induce cell elongation which

eventually led to the transformation in cytoskeletal stress and the differentiation towards osteoblasts.[86] Park *et al.* investigated the cell response on TNTs with different diameters.[12] As Fig. 5A-C shows, TNTs with diameters larger than 50 nm could damage cell adhesion, proliferation and migration, while TNTs with a diameter of 100 nm could give rise to cell apoptosis. The cell adhesion is mediated by the adhesive plaque complex which formed by the aggregation of integrin on cell membrane. As shown in Fig. 5D and E, the cell morphology reveals large osteoclasts only on 15 nm nanotubes and osteoblasts was highest on 15 nm tube diameters, but severely impaired on nanotubes with diameters larger than 70 nm.

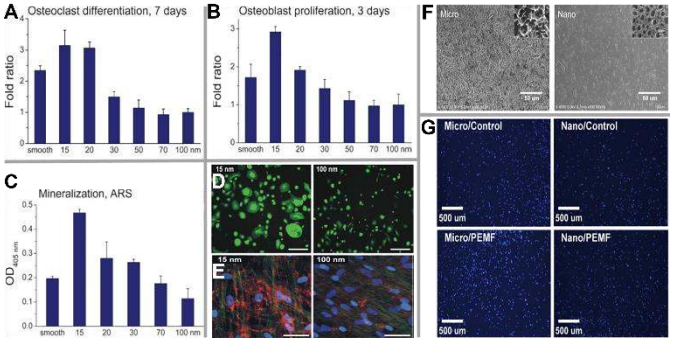

Fig. 5 Size-dependent response of osteoblasts to TNTs including A, B, C. (A) Osteoclast differentiation measured by counting multinucleated cells. (B) Cell proliferation measured by cell counting. (C) Mineralization (alizarin red staining) and osteogenic differentiation measured by osteocalcin expression. (D) Cell morphology reveals large osteoclasts only on 15-nm nanotubes. Adapted with permission from ref. 12. Copyright 2009 Wiley. (E) Primary osteoblasts was highest on 15-nm tube diameters, but severely impaired on nanotubes with diameters larger than 70-nm. (F) SEM images showing the micro/nano topography. (G) Images of osteoblast attachment after 1.5 h of incubation. Adapted with permission from ref. 95. Copyright 2014 Elsevier.

Brammer *et al.* prepared TNTs with different diameters and annealed at 500 ℃.[87] It is obvious that the percentage of spherical cells are higher on nanotubes with diameter of 50, 70, 100 nm than that on the polystyrene, Ti, and the nanotube with diameter of 30 nm. The highest percentage of round cells, was observed on the 70 nm of diameter nanotubes. According to the amount of adhered cells, there is no obvious difference in cell growth on TNTs with different nanotube diameter, but the nanotubes with diameter of 50 nm to 100 nm may increase the production of extracellular matrix (ECM).

4.4.2 Crystalline phase of TNTs

Many studies showed that the crystalline phase of TNTs has an obvious impact on their bioperformance.[88] Park *et al.* indicated that endothelial cells were significantly decreased after 3 days of culture on the surface of anatase when compared with that of amorphous TNTs. Meanwhile, mesenchymal stem cells showed stronger adhesion and higher proliferation rate on the surface of amorphous TNTs. Oh *et al.* showed that the proliferation rate of osteoblasts on amorphous TNTs decreased slightly compared to the anatase phase.[13]

It is found that anatase phase is more beneficial for growth of osteoblast compared with rutile and amorphous phase. Yu *et al.* investigated preosteoblast responses to TNTs annealed at 450 ℃, 550 ℃ and 650 ℃ for 3 h.[89] The result indicated that nanotubes with a mixture of anatase and rutile phase had maximum effect on proliferation, spreading and mineralization of preosteoblast. There are also reports pointing out that rutile and anatase are more advantageous in forming hydroxyapatite in simulated body fluids.[90]

4.4.3 Surface chemical components

The interaction between implant surface and surrounding environment would generate a reaction layer, which is similar to the oxide film of metal surface pollution surface contamination. Surface treatment of Ti could change the chemical components, especially the content of fluorine. The chemical component changes of TNTs could have an obvious influence on cells adhesion, proliferation and differentiation. Park *et al.* reported that the fluorine content of TNTs has a minor effect on early mesenchymal stem cell, but higher fluorine content could improve the cell proliferation after 3 days of culture.[91] Seo *et al.* found that a significant increase in the hydrophilicity of the surfaces as well as changes in the surface chemistry could improve the cell viability, attachment and differentiation.[92]

However, various cells have respective and particular chemical components, more attention is needed on the influence of the TNTs chemical components on different kinds of cells.[93]

4.4.4 Surface charge

Gongadzel *et al*. proposed a mechanism of cell adhesion on sharp edges of nanorough titanium implant.[60] The basic hypothesis was that the attraction between the negatively charged titanium surface and a negatively charged osteoblast is mediated by charged proteins with a distinctive quadrupolar internal charge distribution. According to the results, the nanorough titanium implant had an increased surface charge density and electric field strength due to the curved nanoscale protrusions and edges. Such nanorough regions could obviously improve the adsorption of fibronectin and osteoblastes onto the negatively charged titanium surface.[94]

Pulsed electromagnetic fields (PEMFs) can accelerate osteoblast proliferation and differentiation on implant surfaces by upregulating the expression of relevant genes. Wang *et al.* investigated the influence of PEMFs on the interaction between cells and the titanium surface.[95] As shown in Fig. 5F and G, microscale and nanoscale titanium surfaces were used to culture rat osteoblasts under PEMF stimulation. The amount of adsorbed proteins were significantly improved by the PEMF, and the amount of attached osteoblasts in the PEMF group was substantially greater than that in the control group after 1.5 h culture, which resulted in the formation of more intracellular microfilaments and stress fibers. The results of the study suggest that PEMFs could be used as a potential adjuvant treatment to improve the osseointegration of titanium implants.

4.4.5 Surface wettability

The bioactivity of TiO_2 is affected by its surface wettability in two ways: one is the direct physical-chemical connection between the cell and the surface of the material, and another is the indirect effect on the cell adhesion through adjusting the protein adsorption. The surface wettability is mainly affected by surface chemistry and morphology.

Recent reports demonstrated that hydrophilic surfaces could enhance cell adhesion and proliferation compared with hydrophobic

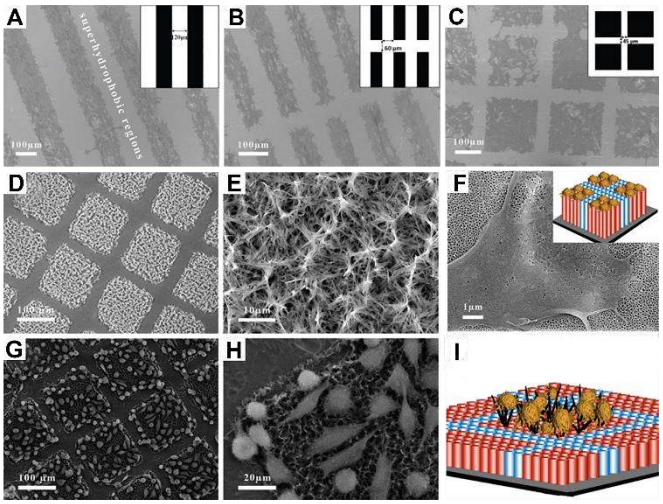

Fig. 6 SEM images of 3T3 cell adhesion on the superhydrophilic–superhydrophobic TNA surfaces micropatterned with distances between superhydrophilic regions were 120 μm (A), 60 μm (B), and 45 μm (C) respectively for 24 h. Insert: the schematic of the corresponding wetting patterns; (D) SEM images of 3D patterned CaP on TNTs surface; (E) maginified SEM of CaP superhydrophilic region; (F) Magnified image of cell on the superhydrophilic area of 2D pattern. The inset: schematic diagram of the site-selective cell layer on 2D TNTs scaffold; (G, H) SEM images of the MG-63 cells adhering on the CaP patterning surface; (I) Schematic diagram of the site-selective cell immobilization on 3D CaP@TNA scaffold. Adapted with permission from ref. 95. Copyright 2013 Wiley.

surfaces.[96] The high surface energy of TNTs increases the early adsorption of protein molecules. It is known that protein adsorption is of great importance in regulating the cell interactions at the implant surface.[97] The anodic TNTs layer is hydrophilic and the wettability can be tuned by changing the nanotube diameter. Bauer *et al.* decorated the surface of TNTs with self-assembled monolayer of n-octadecyl phosphate and the modified TNTs showed a tube-dependent hydrophobic properties.[98]

Recent reports demonstrated that hydrophilic surfaces could enhance cell adhesion and proliferation compared with hydrophobic surfaces. To investigate the effect of wettability, especially superhydrophobic and superhydrophilic surfaces on cellular response, Lai *et al.* fabricated extreme wettability contrast pattern successfully. As shown in Fig 6A-C, 3T3 fibroblast cells were cultured on three different superhydrophilic–superhydrophobic patterned surfaces.[99] It turned out that cell adhesion could be selectively mediated by the superhydrophilic-superhydrophobic patterned surface. Furthermore, to investigate the cell spatial structure for biomedical application, they established three-dimensional CaP micropatterns based on TNTs surfaces.[100] As shown in Fig. 6D, E and G, H, the CaP nanobelts were deposited into the superhydrophilic regions while the superhydrophobic areas were kept intact. MG-63 cells adhered on CaP patterning surface selectively, and the boundary of cell adhesion can be easy observed. Fig. 6F, I shows the schematic diagram of 2D and 3D pattern structure, respectively. Similarly, Huang *et al.* prepared wettability surface by selective coating ink on superamphiphobic anatase hierarchical TiO_2 (AHT) and 3T3 cells were found immobilize on the ink covered amphiphilic regions by a common cell culture process.[101] In addition, it was also found that the micropatterns would support the cell elongation and cell alignment. In contrast, there was no obvious elongation nor orientation on untreated Ti surface.[102] Different methods of disinfection can affect the hydrophilicity and free energy of TNTs surface, which further affect the cell adhesion, extension and differentiation.[103]

4.5 Bone formation on TNTs

TNTs possess improved bioactivity mainly due to the nanoscale featured appearance compared with untreated titanium. They could promote bone integration between implanted materials and surrounding bone tissue by enhancing cell responses,[104, 105] due to the higher wettability of nanoscale surface and increased selective adsorption of proteins from surrounding body fluids.

Previous researches showed that TNTs could not only promote proliferation of osteoblasts *in vitro*, but also attract lots of osteoblasts to TNTs surface *in vivo*.[106] It is well known that osteoblast proliferation is a prerequisite for bone formation, and the function of osteoblasts can be evaluated by the expression of collagen (FMA, MMA, NMA) and osteocalcin (FOC, MOC, NOC). Strong positive staining of collagen [NMA] and osteocalcin [NOC] was found to express actively on TNTs surface. Thus, the surface nanostructured implants are promising for clinical application.

To investigate the influence of nanotubes with different diameters on bone formation, TNTs samples with diameters ranging from 15 to 100 nm were implanted in the frontal skulls of six pigs by Wilmowsky *et al.*[86] Nanotubes with a diameter of 15 nm had lowest bone implant contact (BIC) value, while the value of BIC increased dramatically on those with a diameter of 100 nm. The result of BIC detection indicated that the bone formation increased with increasing nanotube diameter on the implant surface. The peripheral new bone formation of implants is a result of the interactions among various cells, growth factors and cytokines. Furthermore, immunohistochemical stainings were used to estimate the sequential order of the bone-formation and bone regeneration process. The expression of BMP-2 increased with the increasing space between nanotubes, and the amount of type-I collagen decreased with increasing tube diameters. The expression of osteocalcin was higher on large diameter nanotubes (50-100 nm) than small diameters (15-30 nm). Park et al. has verified that nanotubes with a diameter below 30 nm could promote the differentiation of hematopoietic stem cells (HSCs) into osteoclasts, while osteoclast differentiation was dramatically inhibited on nanotube with diameters between 50-100 nm.[12]

Osteogenesis and angiogenesis that have interaction *in vivo* are two pivotal processes for implant osseointegration. Shen *et al.* prepared alendronate (Aln) loaded hydroxyapatite (HA)-TNTs substrates. The vitro study indicated TNTs-HA-Aln substrates can promote the proliferation/differentiation of osteoblasts and inhibit the differentiation of osteoclasts. The vivo study with osteoporotic rabbits showed that TNT-HA-Aln implants can improve local osseointegration compared with other Ti-based implants. The study provided a new insight into the development of functional titanium-based implants for improving early mechanical fixation under

osteoporosis.[107] Bai *et al.* developed silicon (Si) doped TNTs coating which showed good cytocompatibility to both osteoblasts and endothelial cells (ECs). And it was beneficial to improve proliferation, spreading, alkaline phosphatase activity, and matrix mineralization of osteoblasts. Meanwhile, TNA-Si induce better EC proliferation and vascular endothelial growth factor secretion from ECs. In particular, TNA-Si with the strongest osteogenic and angiogenic activities is highly promising as the next generation hard tissue implant coating.[108]

5. Functionalization of TNTs

5.1 Immobilization of biomolecules

Untreated titanium implants have low biological activity, poor bone binding ability and antibacterial property, which may lead to prolonged or even unsuccessful implantation and bacterial infection.[109] A variety of methods have been developed to improve their biological activity, osseointegration and bone regeneration, including physical methods, such as hydrophobic interactions, hydrogen bonds and electrostatic interactions, and chemical treatments, such as the covalent attachment with formation of ether, amide and thioether linkages, and biochemical methods.[110-112]

TNTs can be functionalized by surface modification with various biomolecules. Dip coating and spin coating are the most common coating methods.[113] Spin coating involves applying a solution on a rotating substrate, followed by ejection and evaporation of the solvent. Dip coating is based on immersing the substrate in a solution, followed by gravitational drainage and evaporation of the solvent. Both methods allow a uniform film to be formed on the surface of the substrate.[114] Bone morphogenetic protein-2 (BMP2) could be successfully immobilized on TNTs by covalent binding, which significantly promoted the differentiation of bone marrow mesenchymal stem cells into osteoblasts.[115] Lyophilization has also been applied for filling TNTs with connective tissue growth factor (CNN2).[116]

Various kinds of peptides and proteins can be anchored onto TNTs to improve the osseointegration. Enzymes could be also successfully immobilized to detect specific analytes for bioenergetics. As a

Table 1 Biomolecules that functionalize TNTs, combined method and their main functions.

Biomolecules	Functions	Ref.
Bone morphogenetic protein-2	Promote the ability of bone marrow mesenchymal stem cells to differentiate into osteoblasts *in vitro*	115
Chitosan	Improve drug elution and osteoblast adhesion and enhance bone osseointegration.	118-120
Polydopamine	Extended the release period of drug and maintained a sustained release kinetic.	121, 122
Quercetin	Loads TNTs and its release into the environment as an alternative for the treatment of postoperative infection, inflammation and quick healing with better osseointegration	123
Trehalose	Have osteogenic potential with BMSCs and anti-inflammatory properties on TNTs	124
Gelatin	Improved osteoblast adhesion and propagation and as coating to control drug release condition	125-127
Hemoglobin	Detected the hydrogen peroxide	128
Urate oxidase	Detected the uric acid	129
Glucose oxidase	Detected the glucose	130, 131
poly(3-caprolactone)	Improved the biocompatibility dissolubility and flexibility of the nanotubes	132
Antimicrobial peptides	Possess antimicrobial activity	109, 133, 134
Osteogenic growth peptide	Enhanced osteoblast differentiation	135
Gly-Arg-Gly-Asp-Ser peptide	Enhance cell adhesion and increase cell spreading and proliferation	136
Arg-Gly-Asp peptide	Increased rat bone marrow stromal cells BMSCs adhesion and dramatically enhance the osteogenic gene expression of BMSCs	137, 138
Lys-Arg-Ser-Arg peptide	Increased preosteoblast adhesion and osteogenic gene expression on TNTs	139
Palmitoyl-oleoyl phosphatidyl-choline	Used as a barrier for controlling and sustaining release of drug	133
Epidermal growth factor	Promoted proliferation of MSCs and prevented cellular apoptosis	140
Small interfering RNA (siRNA) targeting tumor necrosis factor alpha (TNF-α)	Improved bone formation and inhibit inflammation	141

biocompatible polyelectrolyte, chitosan can be applied for surface modification with antimicrobial property, and work with the drug loaded in TNTs synergistically.[117] Table 1 summarizes the biomolecules that have been applied functionalize TNTs.

5.2 Metallic nanoparticles

Recently, nanoparticles (NPs) such as silver (Ag), gold (Au), zinc (Zn) and copper (Cu) have been successfully introduced into TNTs to improve their antibacterial activity.[142-144] Ag deposited TNTs exhibit excellent antibacterial activity, and have great application potential in clinic applications with good reusability.[76] Jia *et al*. immobilized Ag NPs to the peripheral surface and the porous lumen of nanotubes by polydopamine reduction, which endowed the TNTs with excellent antibacterial activity against *S. aureus* strains.[145] The antibacterial activity against the early adherence of *S. aureus* was demonstrated by morphological observation after 24 h of culture. It could be seen some of the attached *S. aureus* cells were entrapped within the pores. The interesting phenomenon of "traps kill" bacteria provided researchers with a new idea. Zhao *et al.* reported that Ag NPs modified TNTs exhibited excellent ability of killing the planktonic bacteria, and the antibacterial ability could be maintained up to 30 days.[146] Similarly, Ag NPs were immobilized on TNTs by plasma immersion ion implantation, which created a contact-sterilizable prosthetic surface.[147] Furthermore, dopamine, which served as an adhesion agent of coating and a reductant and diffusion barrier of Ag, was employed by self-polymerization on the TNTs surface, after which silver/calcium phosphate (CaP) composite was immobilized on the surface. The resulting Ag/dopamine/CaP material showed excellent antibacterial ability as well as good biological performance due to the synergistic effects of polydopamine and Ag/CaP. In particular, the top CaP coating would decrease the adverse effect of Ag on proliferation of the osteoblasts. The prepared materials are very promising for biomedical implant applications due to their potential to prevent implant associated infection and promote osteointegration.[148]

Au NPs have a shear effect on the hydrophobic chemical bond under visible light, which can lead to the formation of a "hydrophobic lid" containing gold nanoparticles covered on top of the nanotubes,[149] and the bottom of the nanotubes can be covalently immobilized with the desired antimicrobials by silanization. Under visible light irradiation, nano-gold can shear the covalent bonds between the bottom nanotubes and the antimicrobial agent so that it can realize the responsive release of visible light to the local drug.[150.]

Zn is an important element in the human body, which can promote the synthesis of DNA, enhance enzyme activity and maintain the role of nucleic acid metabolism. The release of Zn ions also has a positive effect on the enhancement of osteoblast adhesion.[151] TNTs loaded with zinc oxide NPs can effectively inhibit the growth of Streptococcus mutans and Porphyromonas gingivalis, meanwhile significantly enhance osteogenic differentiation and osseointegration compared with untreated titanium.[152]

Cu NPs, which can release Cu ions, are expected to play a multiple role in healing burn injuries, preventing infection, and helping the formation of bone matrix.[153] Qin *et al.* indicated that the release of Cu ions is related to a strong antibacterial efficiency against bacteria strains found in wound and skin.[154] Based on these study, Cu NPs were deposited on the nT-TiO_2 surface, which were deemed to improve osteoblast adhesion and resulted approximately 100% antibacterial rate against *Escherichia coli* (*E. coli*) and *S. aureus*.[155]

The Zn/Ag couple formed on Zn/Ag dual-ion co-implanted titanium showed good osseointegration and antibacterial property *in vivo* used a rabbit tibia model.[156] It is reported that the osteogenic and antibacterial properties of Mg/Ag dual plasma treated titanium were better than that of single plasma treated Ag or Mg groups.[157]

5.3 Deposition of Hydroxyapatite

Electrodeposition, hydrothermal treatment, wet chemical synthesis and physical vapor deposition methods are commonly used to deposit HA onto the surface of TNTs.[158-160] The mechanism of HA growth on TNTs in simulated body fluid (SBF) is caused by the dipolar nature of the TiO_2/HA interface. OH^- could be adsorbed from SBF to form Ti-OH groups. Ti-OH groups are negatively charged because of the presence of deprotonated acidic hydroxides when the pH = 7.4. Negatively charged TNTs can adsorb Ca^{2+} from SBF and react with $HOPO_4^-$ or $H_2PO_4^-$ to form calcium phosphate.[161]

Kar *et al.* prepared HA coated TNTs by a pulsed electrodeposition method. The alkaline treatment before electrodeposition provided TNTs with a template for the nucleation of HA inside the nanotube, which increased the bonding strength of the HA coating.[162] Furthermore, HA doped with Ag coated TNTs were achieved by physical vapour deposition to inhibit the adhesion of microorganisms.[163] Hexagonal prismatic HA crystals could also be synthesized by a hydrothermal method using TNTs and urea.[164]

5.4 Drug delivery

TNTs with controlled pore size and depth have been demonstrated to be a promising platform for local drug delivery, and can serve as suitable carriers for various therapeutics, including growth factors, antibacterial agents, anticancer drugs and metal nanoparticles.[79, 165-169] TNTs lumens as a good drug storage bin can be loaded with appropriate antibiotics to prevent implant-related infections.[73] Antibiotics loaded in TNTs could be released locally, which avoids the adverse reactions and low local drug concentration caused by systemic treatment.

Though the tube length of TNTs has no significant effect on the biological behavior of the cells, it mainly influences the drug loading and controlled release from the nanotubes. TNTs may have defects such as early burst of drug and short acting time. The release mechanical of drugs from TNTs includes passive release and intelligent controlled release, according to the difference between antibacterial principles optimized by the surface of TNTs and the way of drug release. The passive release mode is often uncontrollable and have difficulty in preventing local infection. As in the intelligent controlled release mode, drugs in TNTs can be released under the trigger of certain conditions and achieve a variety of programmed drug release, or released intelligently according to the type of pathogenic bacteria through special modifications.[170] And intelligent controlled release of drugs could also be triggered by light, temperature, ultrasonic stimulation and radiofrequency magnetism release.[171, 172] The prepared TNTs are immersed in some antibiotics with different concentrations, and drugs can be loaded into the nanotubes by freeze drying.[173] The multi-drug delivery system, visible light triggering drug controlled release system and the contact/release

dual disinfection system all belong to the intelligent controlled release of drugs on the surface of TNTs. Local multi-drug combination therapy have a positive effect on the treatment of bacterial infections and inflammation elimination, and could improve implant osteointegration and promote bone healing. In order for the loaded therapeutic agents to have extended release, the drugs encapsulated in micelles or nanotube matrix can be coated with a biopolymer, which prevents the rapidly eluting of drugs.[120, 174]

Polymer micelles are a family of thermodynamically stable colloids formed by the self-assembly of amphiphilic block copolymers in water. As a drug carrier, polymeric micelles have two functions: multiple drug loadings and continuous controlled release. D-α-tocopherol polyethylene glycol 1000 succinate (TPGS) is an amphiphilic polymer micelle that has a hydrophilic outer surface and an inner hydrophobic core that acts as a drug carrier for water-insoluble drugs such as indomethacin and itraconazole. In contrast to TPGS, methoxy-polyethyleneglycol 2000 (DGP 2000) has a hydrophobic outer surface and a hydrophilic inner that serves as a carrier for soluble drugs such as gentamycin sulfate.[175] Fig. 7A and B illustrates how to prepare such coatings and micelles using biological molecules such as chitosan and d-alpha-tocopheryl polyethylene glycol 1000 succinate (TPGS), respectively.[119, 176] Furthermore, functionalization of nanotube surfaces is crucial for the preparation of drug delivery nanosystems with high drug loading and sustained release with high *in vivo* biocompatibility and bioavailability. Huang *et al.* prepared two kinds of long-acting drug delivery nanoclusters Enro-NH_2-TNTs and Enro-SH-TNT by combining the surface modification of titanium dioxide nanotubes with the pH adjustment process.[177] Fig. 7C exhibits the process of preparation of loading enrofloxacin (Enro).

Currently, various types of antibiotics are used to enhance the antibacterial property of bone implants, which result in many drug-resistant strains that are more resistant to conventional types and doses of antibiotics. In recent years, the use of natural extracts to combat bacterial infections has drawn much attention.[178, 179] Rhodotrosin is a kind of carotenoid produced by a strain of Rhodotorula and possesses excellent antioxidant and antibacterial properties, Rhodotorula can be covalently bonded with the lumen of TNTs through polydopamine.[180, 181] Compared with pure titanium and drug-free TNTs, those covalently charged with rhodotensin have significantly promoted the surface antibacterial activity of the implants and enhanced the inhibitory efficiency of *E. coli, S. aureus*, Enterococcus faecalis, Bacillus, Pseudomonas aeruginosa and other bacteria. Furthermore, in order to obtain a stable drug release, metal nanoparticles with eminent antibacterial efficacy can also be loaded into nanotubes.[182]

6. Applications

TNTs are widely studied for potential biomedical applications in several fields, including bone therapy, dentistry, cardiovascular stents and biosensor.

6.1 Bone implants

Bone-related diseases have a significant impact on the quality of human life. With the development of society, more and more biomaterials have been used in orthopedics such as artificial joints,

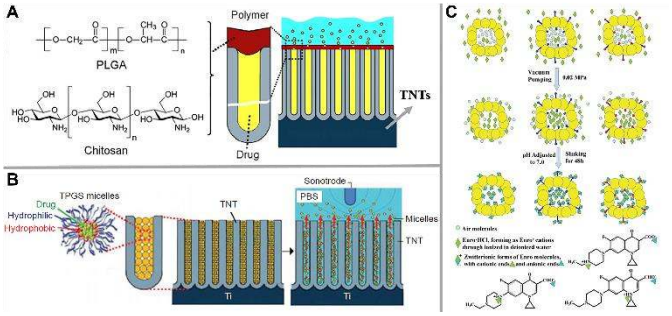

Fig. 7 (A) Chitosan or PLGA polymer film coated on TNT by dip coating; (B) Drugs have been encapsulated in micelles polymeric micelles as drug carriers; Adapted with permission from ref. 177. Copyright 2014 Royal society of chemistry. (C) The process of loading enrofloxacin to form drug delivery nanosystems. Adapted with permission from ref. 177. Copyright 2014 Royal society of chemistry.

spinal fusion, fracture fixation devices (including internal fixation, external fixation) and so on.[183, 184] Biomedical materials used in clinics should possess good biocompatibility, abrasion resistance, corrosion resistance and antibacterial properties.[185, 186] Titanium and its alloys display poor osteoinductivity and antibacterial properties *in vivo*, which affects their long-term lifespan as an endophyte. As one of the promising treatments, TNTs surface modification can improve the surface area and porosity of titanium materials by the formation of highly ordered surface nanostructure with unique physical and chemical properties.[187]

Micro-nano structure is of great significance for promoting the integration and stability of implant and preventing transplant failure.[188] Micro surface structure is conducive to bone cell adhesion and reproduction and further promotes bone conduction and mechanical binding with the surrounding bone tissue.

After the implant is implanted into the bone, it is bone marrow-derived mesenchymal stem cells (BMSCs) which are first recruited to the surface of the implant to participate in the synostosis, and osteoblasts which are derived from the osteogenic differentiation of BMSCs, and subsequently involved in osteogenesis.[189] Studies have shown that TNT arrays can promote osteoblast adhesion, proliferation, differentiation, and the osteogenic differentiation of bone marrow-derived MSC.[190, 191] TiO_2 is a bio-inert material that is not able to chemically bond with the host bone, while HA bioactive coating can form bony union with bone tissue and greatly shorten bone healing time.[192]

Bone implants primarily refer to orthopedic prostheses, such as bone grafts, bone plates, fins, fusion devices and orthopedic fixation devices. as the fixation devices include interference screws in the ankle, knee, and hand regions, stems and pins for fracture fixation, screws and plates for craniomaxillo facial repair, and bone tissue engineering scaffolds for fractures and implants as autologous bone graft or allograft bone graft.[193] Although traditional prosthetic knee, hip, and plate implants are still the most implantable commercial devices, a great deal of research activity has been initiated over the past decade. The principle behind the application of nanotechnology on bone tissue engineerin, which is related to fracture healing. And reverse rotation torque is currently recognized as a method of evaluating osseointegration of implants. The better the

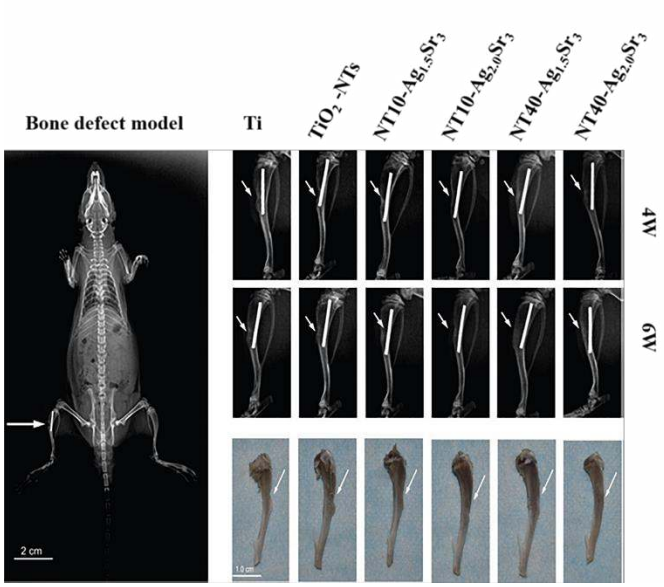

Fig. 8 shows the evidence of healing of bone defects in rats implanted with various Ti surfaces for 4 and 6 weeks [NT10 = TNTs at 10 V, 1 h; NT40 = 40 V, 40 m; Sr_3 = Sr-incorporated TNTs, $Ag_{1.5}$ = soaked in 1.5 M $AgNO_3$, $Ag_{2.0}$ = soaked in 2.0 M $AgNO_3$]. Adapted with permission from ref. 194. Copyright 2016 Elsevier.

osseointegration between implant and bone tissue, the greater the torque required to unscrew the implant.

Cheng *et al.* fabricated strontium (Sr) and Ag loaded TNTs with different tube diameters by hydrothermal treatment to repair rat tibial defect. Fig. 8 shows the bone defect model of rat tibial, the healing process and formation of apparent new bone could be detected at 4 weeks and 6 weeks after the surgery respectively.[194] In order to achieve local bone-targeting delivery system, Liu et al. successfully constructed a new dual-controlled system by loading tetracycline grafted simvastatin (SV) loaded polymeric micelles in TNTs.[195] Fig. 9A and B shows the new bone formation around the middle tibial implants with different surfaces of normal and ovariectomized rats after several weeks implantation, which demonstrated the tightest anchorage of the NT-SVTCPM1 implant and increased thickness of new bone with time.

In addition to the tibia implant model, TNTs are also used in treating cranial defects. Shao et.al used icariin treated titanium particle and induced osteolysis for cranial defects implantation, which proved that icariin can be a new therapeutic candidate for the prevention and treatment of aseptic loosening.[196] Fig. 9C and D presents the prevention of mouse calvarial osteolysis by Ti-particle-induced icariin. As we can see, the mice treated with high concentration of icariin particles induced significantly lower osteolysis than those treated with low concentration and pure Ti particles. Quantification of bone parameters confirmed that the proper concentration of icariin could prevent the loss of osteolytic bone effectively. Furthermore, Kim and Aghaloo *et al.* also did some research about the cranial defects in rabbits, which showed similar results.[197, 198]

6.2 Dental implants

The concept of "bone union" was first proposed by Professor Branemark in 1969, which has become an important theoretical basis of modern oral implants. For patients with bone loss, osteoporosis, diabetes or long-term smoking, the repair of implant prosthesis has many problems such as slow soft tissue healing, hard bone forming on implant interface and peri-implant inflammation.[199-201] Many methods such as large particle blasting, anodizing, acid etching, titanium coating, microarc oxidation, laser cladding, sol-gel, hydroxyapatite coating, protein bioactive coating and antibacterial coating, have been applied to the surface modification of implant in laboratory and clinical studies.[202]

The micro/nanostructures of dental implants and the mechanism of contact with surrounding tissue are similar to those of bone implants. Osteoblasts and other cells associated with osteogenesis around implants are crucial to the formation of favourable osteointegration.[203] Periodontal tissue is not only an important supporting tissue for the teeth, but also helps to balance and repair the surrounding tissue. Human periodontal ligament stem cells (hPDLSCs) are adult pluripotent stem isolated from the periodontal ligament.[204] It has been reported that hPDLSCs have the ability of osteogenic, adipogenic and neurogenic differentiation.[204-206] Li *et al.* have proved that TNTs could promote the osteogenic differentiation of hPDLSCs. PDLSCs on TNTs exhibited much more stretched morphology and higher proliferation rate, and could significantly up-regulate osteogenesis-related markers at both gene and protein levels compared with Ti substrates.[207]

TNTs can be successfully fabricated on blasted, screw-shaped titanium implants via electrochemical anodization technique (Fig. 10). Studies on animals showed that the TNTs screw implants in rabbit femurs demonstrate significantly increased osseointegration strengths and new bone formation, and reveal frequently direct bone cell contact at the bone implant interface as compared with the normal blasted implants.[208] Monetta *et al.* investigated the electrochemical impedance spectroscopy characterization of TNTs surface modified dental implant screws in Hank's solution, and found that the TNTs surface could increase the corrosion resistance of the implant and possess a more active role with promoted formation of chemical compounds containing Ca and P, which further help osseointegration of the dental implants.[209, 210] As shown in Fig. 11A-F, Jang *et al.* prepared TNTs with diameter of 70 nm and length of 5 μm on miniscrew surface. After implanted in the tibias of New Zealand white rabbits for 8 weeks, TNTs on the surface of miniscrews were found to have enhanced osseointegration and improved the stability of the miniscrew.[210] Furthermore, they prepared ibuprofen loaded TNTs miniscrews, and the results showed that ibuprofen-loaded miniscrews had a significantly higher bone-to-implant ratio compared with conventional miniscrews.[211]

There are two main types of dental implant infection: peri-implant mucositis and peri-implantitis.[212] In order to reduce the incidence of implant-related infections and to enhance the anti-bacterial properties of the implant at the gingival margin, it is particularly important to select and load the appropriate antibiotics or antibacterial agents. TNTs were used as a carrier of gentamicin by using electrochemical etching technology, and then coated with chitosan and polylactic acid by dipping coating.[213] The treated TNTs possessed an excellent

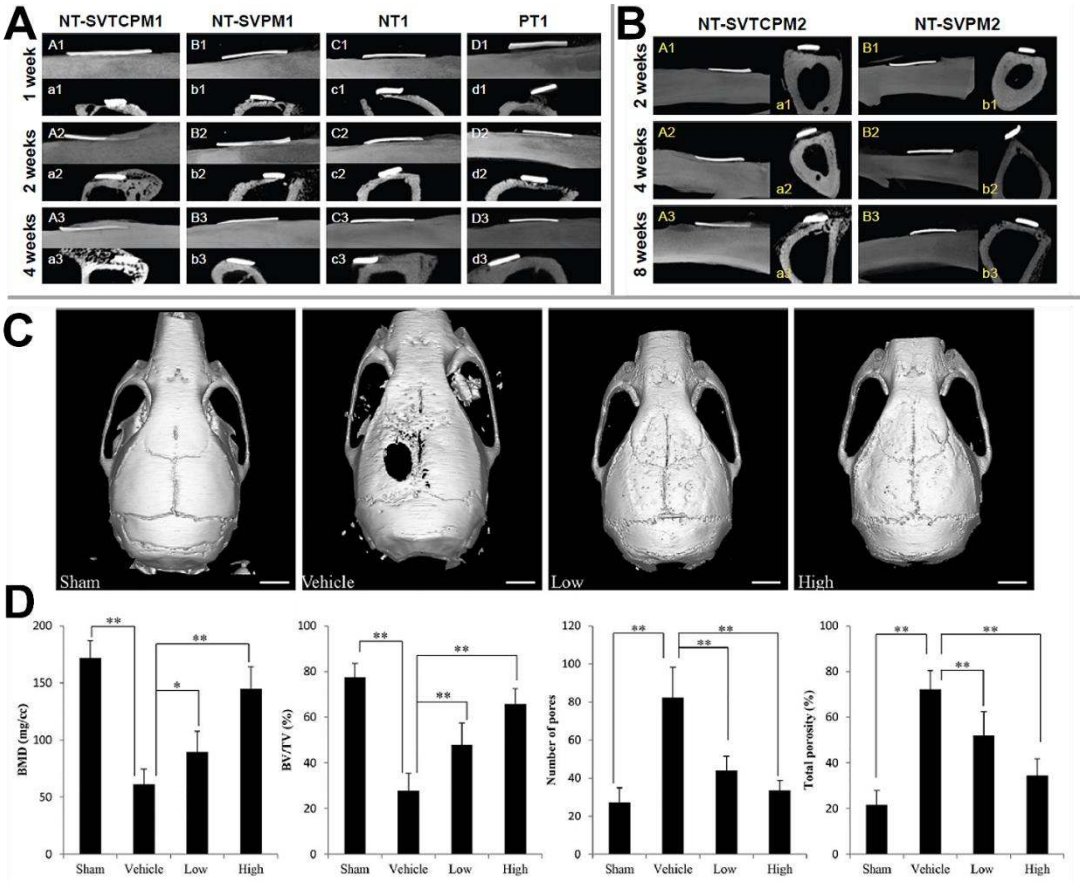

Fig. 9 M-CT images for implant–bone integration around the implant site for implants with NT-SVTCPM, NT-SVPM, NT, and PT surfaces in normal rats (A) and ovariectomized rats (B) at 1, 2, and 4 weeks after implantation (A1-D1, A2-D2, and A3-D3 for the sagittal view of complete 3D images; a1-d1, a2-d2, and a3-d3 for cross-sectional 2D screenshots) [2D, two dimensional; 3D, three dimensional; BV, bone volume; m-CT, microcomputed tomography; NT, uncoated TNTs; NT-SVPM, TNTs loaded with SV-loaded PECL micelles; NT-SVTCPM, TNTs loaded with SV-loaded TC-grafted PECL micelles; PCL, poly(ε-caprolactone); PECL, PEG-PCL; PEG, poly(ethylene glycol); PT, polished Ti; SV, simvastatin; TC, tetracycline; Ti, titanium; TV, total volume.]. Representative mCT 3D reconstructed images obtained from each group (Scar bar = 5 mm) of icariin prevented Ti-particle-induced mouse calvarial osteolysis. Adapted with permission from ref. 195. Copyright 2016 Dove Medical Press. (C). Bone mineral density (BMD), bone volume against tissue volume (BV/TV), number of pores and the total porosity of each sample were showed in (D). Adapted with permission from ref. 196. Copyright 2015 Elsevier.

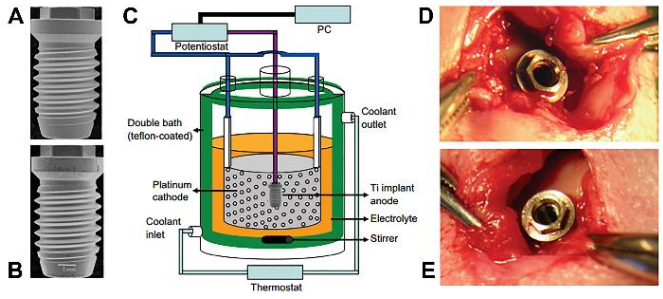

Fig. 10 Macroscopic images of (A) the TiO_2 nanotube-fabricated test implant (B) the blasted control implant. The thread pitch is 600 µm. (C) Schematic of the experimental setup used for the electrochemical nanofabrication. (D and E) One nanotube implant and one blasted implant were inserted in the femur condyle close to the knee joint of each rabbit. Adapted with permission from ref. 208. Copyright 2010 Dove Medical Press.

antibacterial effect and obviously promoted osteoblast adhesion. Gentamicin loaded TNTs could also be prepared by equal channel angular pressing (ECAP) and anodizing technique.[214] Ag NPs have already been widely used in clinical practice.[215, 216] Previous studies have confirmed that TNTs with large diameter can promote the adhesion and proliferation of human gingival fibroblast, meanwhile provide beneficial conditions for the loading of Ag NPs.[173]

A new implant system named Nobel Active™ represents an important milestone for immediate loading, which is an important goal of implantable prosthesis technology.[217] From Fig. 11G and H, it can be seen that the remarkable bone healing before and after regular inspection after several months.

In order to investigate the effect of zirconia-modified TNTs on bone regeneration of dental defects, Benic *et al.* investigated treatment effect of TNTs modified with ZrO_2, deproteinized bovine bone mineral (DBBM) and collagen membrane (CM) in maxilla with semi-saddle bone defects.[218] The area of new mineralized bone and residual bone substitute within the augmented area was showed in Fig. 11I. The application of DBBM particles and collagen membranes revealed

the most favorable result with respect to the enhanced ridge profile for peri-implant defects of zirconia implants.

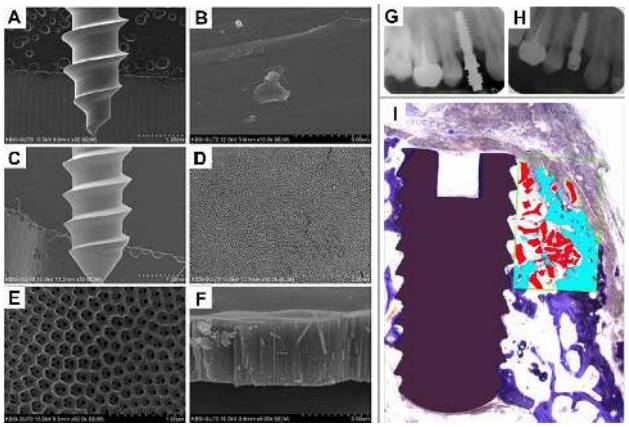

Fig. 11 FESEM images of the miniscrews (A, B) before and (C-F) after anodic oxidation. Adapted with permission from ref. 210. Copyright 2015 Springer. M-CT images of dental implant by traditional impression technique (G) and regular examination after 3, 6, 12 months (H). Adapted with permission from ref. 217. Copyright 2008 Springer. (I) Histomorphometrical analysis of the augmented area (AA) within the former bone defect, the area of new mineralized bone (blue surface) within AA, and the area of residual bone substitute (red surface) within AA. Adapted with permission from ref. 218. Copyright 2017 Wiley.

6.3 Cardiovascular Stents

Cardiovascular diseases were seen as the major cause of death and disability in the world.[219] Atherosclerosis is a kind of inflammatory disease, which may cause serious heart failure and stroke.[220] Though stent implantation is a promising strategy to cure atherosclerosis disease, it would provoke a sequence of cell response and biochemical events.[221] Since cardiovascular stents are planted into the artery, the patients are at a high risk for restenosis inside the vessel at the stented site due to the lack of endothelialization.

Rapid endothelialization after stent implantations can increase the success rate of surgery by decreasing the formation of thrombosis and shortening anticoagulative therapy duration.[222] Besides preventing thrombosis, the ECs can accelerate the differentiation of vascular smooth muscle cells (VSMCs). Actually, VSMCs would drop the phenotype of differentiation when the ECs were corroded. Be in an undifferentiated stage, VSMCs show a proliferative phenotype and achieve cell division, which would cause intimal hyperplasia and further leads to restenosis or vessel blockage.[223] Therefore the investigations, which focus on the direct effect of topography on VSMCs proliferation and phenotype, are very important for avoiding stent graft failure. Based on above, Peng *et al.* investigated the effect of TNTs surface on vascular cells including EC and VSMCs.[224] The result suggested that the topography has a significant influence on the response of EC and VSMCs. TNTs layer could promote the proliferation of EC and secretion of prostaglandin I2 (PGI2) as well as proliferation of VSMCs and expression of smooth muscle a-actin.

However, the process of endothelialization is limited by the growth microenvironment of vascular ECs, such as the topology of the device surface, extracellular matrix (ECM) environment etc. The

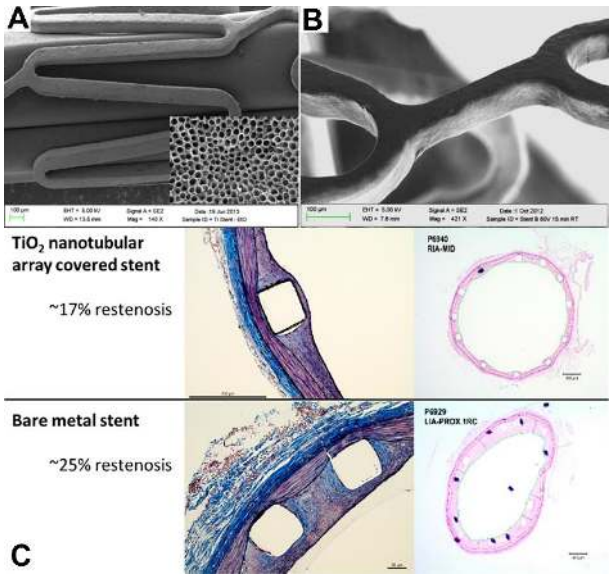

Fig. 12 (A) Complete strut coverage by TNTs of a crimped stent onto a balloon. Inset: Nanotubes, average nanotube diameter is 90 nm. (B) TNT array covered stent. SEM revealed full TNTs coverage. No critical damage at bridges, struts, or turns was observed. (C) TNTs covered stent showed a statistically significant reduction of stenosis compared to SS stent. Adapted with permission from ref. 231. Copyright 2017 American Chemical Society.

defined micro-patterns, which were usually used to simulate the natural vessel, can inhibit the VSMCs to contractile phenotype.[225] The contractile phenotype, which is the physiological status of VSMCs, would generate ECM, establish the excellent growth environment of ECs, and promote ECs proliferation.[226] Yang *et al.* proposed a strategy for the BVLD-eluting TNTs system creates a favorable microenvironment by using poly-dopamine to tailor the surface functionalities of TNTs.

The combination of the biological functions of the BVLD and TNTs provided the multiple functions of improved hemocompatibility and selectivity for endothelial cells (EC) in a competitive growth with VSMCs.[227] However, the generation of autologous SMCs may do patients harm, and the vitro SMCs culture is hard to control while immune rejection and inflammation need to solved.

MSCs were known as be nonimmunogenic, and can be separated from various tissues. [228, 229] Li *et al.* investigated the proliferation of MSCs on micro/nanostructured TiO_2 surface.[230] The result indicated that both micro and nano TiO_2 with anatase phase had excellent cytocompatibility, and could promote MSC proliferation, elongate MSCs and regulate oriented growth of MSCs. In addition, the differentiation of MSCs into contractile SMCs induced by the micro/nano surface could further be ascribed to the attachment and proliferation of ECs. In conclusion, this study build a foundation for the interface functionalization of the cardiovascular stents.

However, more studies are needed to focus on the *in vivo* experiments to evaluate their feasibility. Nuhn *et al.* firstly investigated the potentially beneficial effects of TNTs on vascular tissue *in vivo*. Stents were commonly deployed using balloon catheters in interventional cardiology. The stent with width of the turns and bridges of 90 μm have ability of folding and expanding homogeneously. As shown in Fig. 12A and B, the TNTs grow

vertically to the substrate surface, and no adverse influences for TNTs stability were observed. TNTs remained intact after crimping and inflation by visual inspection of stents. The stents were then implanted into the iliofemoral artery using an over inflation model in rabbit, as shown in Fig. 12C, both stainless steel (SS) and TNTs stents maintained the widely expanded state within the iliofemoral arteries. The percent area stenosis of SS stents and TNTs stents was 24.76% ± 7.45% and 17.22% ± 1.11%, respectively. Compared with the restenosis rates of SS stents, the restenosis rates for TNTs stents were 30.45% lower. Therefore, TNTs surface modification is a promising approach to keep stent patent for a long-term use and to address in-stent restenosis issue.[231]

6.4 Biosensors

6.4.1 Detection of glucose

With the increased number of diabetes cases worldwide, the accurate detection of glucose become more and more important. Recently, TNTs have been used as a biosensor for the detection of glucose oxidase (GOD). Xie *et al.* fabricated an electrocatalysis system, in which GOD was embedded inside the TNTs channels and pyrrole was electropolymerized for quantitative detection of H_2O_2 and glucose.[232] The obtained biosensor showed high response sensitivity and low detection limit. As the Fig. 13A shows, the steady time for indirect detection of glucose by GOD-TiO_2/Ti was prolonged compared with that of pure TiO_2/Ti electrode. Furthermore, Prussian blue (PB) nanocrystals were deposited onto TNTs surface and the GOD/Au NPs nanobiocomposites are subsequently immobilized into the nanotubes via electrodeposition.[131] As shown in Fig. 13B and C, the obtained electrode exhibited a fast response in a wide linear range and excellent stability to UA/AA/AP as well as great sensibility. As shown in Fig. 14A, Zhu *et al.* prepared the composite of a polyaniline (PANI) and TNTs and then was used to immobilize GOD for the development of electrochemical biosensor. The current of PANI-TNTs modified GOD biosensor increased by 55% compared to TNTs biosensors. This is attributed to the improved properties of the composite.[233]

Though enzymatic glucose sensors possess advantages such as excellent selectivity and low detection limit, their applications are still limited by the instability, complex enzyme immobilization and high sensitivity to temperature, pH, and humidity.[234] To overcome these disadvantages, many studied focused on non-enzymatic glucose sensors and different methods of glucose response determination. Furthermore, Pt, Au, Pd, Ni nanoparticles have also been reported to be deposited on TNTs during sensor development.[235-239] For examples, Yu et al. developed a nonenzymatic glucose sensor based on Ni nanoparticles-modified TNTs surface (Ni NPs/TNTs) using pulsed electrodeposition method (PED). The detection limit of this sensor towards various concentrations of glucose at 0.6 V in 0.1 M NaOH solution are shown in Fig. 13D.[240] Cai *et al* developed a nonenzymatic blood glucose sensor based on Pt, Au, and Pd NPs constructed with the assistance of polydopamine on TNTs.[241]

However, there are still some problems in metal NPs modified TNTs electrode, such as insufficient sensitivity and stability. Considering the advantages of bimetallic such as good electrocatalytic activity and enhanced stability.[242] Li *et al.* prepared Ni-Cu/TNTs electrodes used for non-enzymatic glucose detection in alkaline electrolyte solution. The Ni-Cu/TNTs electrodes exhibited excellent electrocatalytic activity compared with Ni/TNTs or Cu/TNTs electrodes.[243]

6.4.2 Detection of H_2O_2

The sensitive detection of hydrogen peroxide (H_2O_2) is of great importance to many fields such as environmental analysis, food process, chemical, biochemical and pharmaceutical industries.[244] Many methods have been proposed for the determination of H_2O_2 consisting of flourometry, spectrometry, chemiluminescence, titremetry, electrochemical and chromatography methods. Among these methods, electrochemical sensors possess several advantages, such as fast analysis, low cost, high sensitivity and selectivity. Many kinds of enzymes-based electrochemical sensors for the detection of H_2O_2 have also been proposed.

Even though all kinds of peroxidases possess enzymatic activity, horseradish peroxidase (HRP) is the most usually applied enzyme in the evolution of enzymes-based electrochemical H_2O_2 biosensors. Liu *et al.* investigated the coadsorption of HRP and thionine (Th) on TNTs to produce a new H_2O_2 sensor.[245] They placed the electrode into phosphate buffer (PB) at 4 °C for 2 weeks, and it maintained 86% of the initial current response. Furthermore, Kafi *et al.* developed a promising H_2O_2 sensor through the co-immobilization of HRP and chitosan onto Au-modified TNTs.[246] The electrochemical measurement indicated that the Au modified TNTs could be used as great matrices for the immobilization of HRP, and the obtained biosensor showed long linearity, low detection limit, high stability and very good reproducibility.

There were some studies focused on the co-detection of glucose and H_2O_2. For example, modified TiO_2 layers were deposited on Si substrate by metal organic chemical vapour deposition or sol-gel methods, then two different enzymes, GOD and HRP were immobilized on electrode surface by dip-coating technique.[247] The GOD/HRP/TNTs electrode could serve as a sensor for detecting both glucose and H_2O_2. It exhibited direct voltammetric responses, good sensitivity, low detection limit (about 10^{-6} M) and fast time response (few seconds), which make these electrodes good candidates for low-cost, miniaturized multi-tasking biosensors.

Though the HRP based sensors have lots of advantages such as high sensitivity and selectivity, there are still several drawbacks including relatively slow electron-transfer processes, low activity and high cost.[248, 249] Alternately, hemoglobin (Hb) or cytochrome c peroxidase (CcP) can be used to replace HRP due to its better properties. For examples, An *et al.* achieved efficient direct electron transfer (eT) of Hb immobilized onto pristine TNTs by controlling location and distribution of Hb.[250] In addition, Hb-in-TNAs could be applied as H_2O_2 sensor due to its higher electro-catalytic bioactivity and shorter response time. The H_2O_2 sensor showed a wide detection range from 10^{-8} to 10^{-3} M and a detection limit of as low as 7.0×10^{-8} M. There are several researches focused on the the co-immobilization of Hb and TNTs.[128, 251] In addition, Au nanocrystal (Au NCs) were introduced into TNTs surface by one-step electrodeposition to form Au NCs/TNTs hybrids, it showed better promotion for direct electrochemistry. [252] The subsequently immobilized cytochrome c (Cyt c) exhibited favorable electrocatalytic activity toward the reduction of H_2O_2. Moreover, it could be adapted to different pH circumstances ranging from 3 to 8 with good response and resolution,

which is a promising candidate for the third-generation biosensors. The performance of the above mentioned glucose and H_2O_2 biosensor was listed in Table 2.

Table 2. Comparison of the performance of different glucose biosensors.

Electrode	Type	Detection limit (μM)	Linear range (mM)	Sensitivity ($\mu A\ mM^{-1}\ cm^{-2}$)	Ref.
GOD/ pyrrole/ TNTs	glucose	2	-	45.5	160
GOD/PB/Au NPs /TNTs	glucose	3.2	0.01-0.7	0.248	161
GOD/BSA/ TNTs	glucose	3.8	0.05-0.65	199.6	162
Ni NPs/TNTs	glucose	2	0.004-4.8	700.2	168
Pt NPs /dopamine/ TNTs	glucose	20	0.1-4.5	56.0	168
Ni-Cu/TNTs	glucose	5	0.01-3.2	1590.9	171
HRP/Th/TNTs	H_2O_2	1.2	0.011-2	-	173
HRP/chitosan/Au NPs/TNTs	H_2O_2	2	0.005-0.4	-	174
GOD/HRP/TNTs	H_2O_2	1	0.005-0.55	-	175
Hb/TNTs	H_2O_2	0.07	0.01-10	0.919	178
Au NCs /Cyt c /TNTs	H_2O_2	1.21	0.002-0.349	-	181

6.4.3 Detection of photoelectrochemical biomolecule

TNTs materials have attracted great interest in the emerged photoelectrochemical (PEC) bioanalysis due to its desirable properties including good biocompatibility, chemical/thermal stability and excellent sensitivity.[253, 254] α-Synuclein (α-SYN), which is a very important neuronal protein, can be used as a marker for Parkinson's disease. Mandal *et al.* demonstrated an electrochemical sensor for the rapid detection of myoglobin level in blood. The result reveal that the TNTs surface not only decreases the background current response but also helps in the facile electron transfer to the underlying electrode. The enhanced electrochemical response generated by denaturing the protein also improved the efficiency of analytical.[255] An *et al.* prepared a low-cost and sensitive PEC sensor based on the Au-modified TNTs for the detection of a-SYN.[256] Moreover, the antibodies (Ab1) with high stability and bioactivity was used to fix target a-SYN, while the GOD was used to improve the sensitivity. The study showed that this sensor possessed high sensitivity, stability and reproducibility, and is therefore promising for protein detection.

The accurate quantification of heart proteins cardiac troponin I and T is the major way to the diagnosis of acute myocardial infarction (AMI). Traditional assay methods are not sensitive enough in the first few hours due to the obvious delayed occurring between the onset of ischemia and the increase in serum concentration of cTns. Kar *et al.* developed a highly sensitive fluorescence immunoassay method, in which robust and ordered carboxyalkylphosphonic acid self-assembled monolayers modified TNTs were used.[257] The process can be visualized in the schematic in Fig. 14B, and the sensor can detect a concentrations of human cardiac troponin I as low as 0.1 pg/mL.

A novel sensitive detection for vascular endothelial growth factor (VEGF) were fabricated with p-type BiOI nanoflakes (NFs) array and n-type TNTs array.[258] The configuration of obtained BiOI NFs array/TNTs array possessedgreat excitation efficiency and excellent photoresponsibility due to the unique structure and the synergy effect of photoelectrochemistry in the formed p-n junction. This study not only proposed a system for VEGF detection, but also created a completely different view for PEC biomolecular detection.

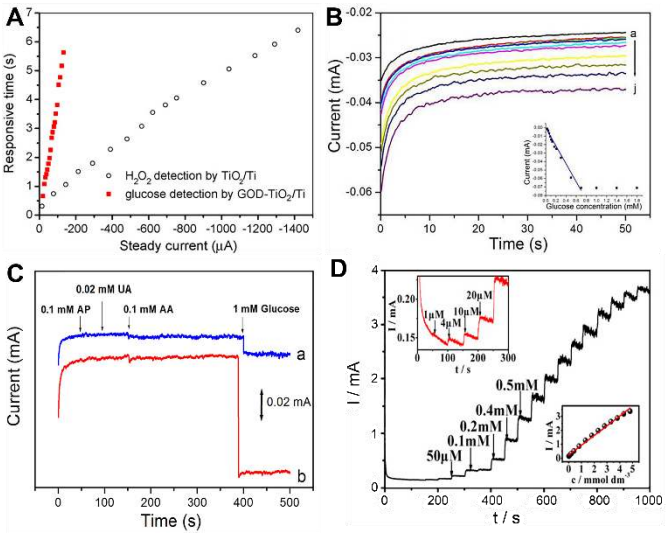

Fig. 13 (A) Responsive time in terms of steady current for direct detection of H_2O_2 by TiO_2/Ti and indirect detection of glucose by GOD-TiO_2/Ti electrode. Adapted with permission from ref. 232. Copyright 2007 Elsevier. (B) GOD-PB/Au NP/TNTs electrode (a) in the absence and (b-j) successive addition of glucose at 20.35 V; inset shows the linear calibration plot. (C) Amperometric response of the GOD-PB/Au NP/TNTs (curve a), and (GOD/Au)-PB/Au NP/TNTs (curve b) based electrodes for the addition of 0.1 mM AP, 0.02 mM UA, 0.1 M AA and 1.0 mM glucose at 20.35 V to air-saturated PBS. Adapted with permission from ref. 131. Copyright 2014 Springer Nature. (D) Typical amperometric response of activated Ni-NPs/TNTs towards various concentrations of glucose at 0.6 V in 0.1 M NaOH solution; left inset: the amplified response curve, right inset: the linear calibration curve. Adapted with permission from ref. 240. Copyright 2012 Elsevier.

The detection of L-lactate can provide key information for clinical diagnostics, medicine validation, and food analysis.[259-261] Therefore, various electrochemical biosensors have been developed for the accurate and fast detection of L-lactate. As Fig. 14CI shows, Zhu *et al.* prepared a ternary composite consisting of TNTs, PANI and gold nanoparticles (GNPs) for photoelectrochemical (PEC) biosensor. In detail, the PEC reaction mechanism of L-lactate at TNTs-PANI-GNP was displayed in Fig. 14CII, LDH catalyzed the transformation of lactate to pyruvate with the aid of NAD^+, which was converted to NADH simultaneously. The increase of lactate concentration in the test solution produced more NADH, which would consume more photoexcited holes and therefore generate larger photocurrent for quantitative determination of lactate.

6.5 Brain Tumors

Systemic chemotherapy, as a usual method to treat brain tumors, has inherent disadvantages that limit the clinical effectiveness.[122] To overcome these limitations, localized chemotherapy is the best treatment method, especially for malignant glioma. Kalbacova *et al.* demonstrated that TNTs layers can be used as a photocatalyst for killing cancer cells.[262] The vitality of cancer cells cultured on TNTs layers was significantly decreased, and the shape and size of cells were obviously affected. They also proposed a possible application for anticancer treatment that using a focused UV light as excitation source to trigger photocatalytic reaction on TNTs. The excitation source also can be X-rays.[263]

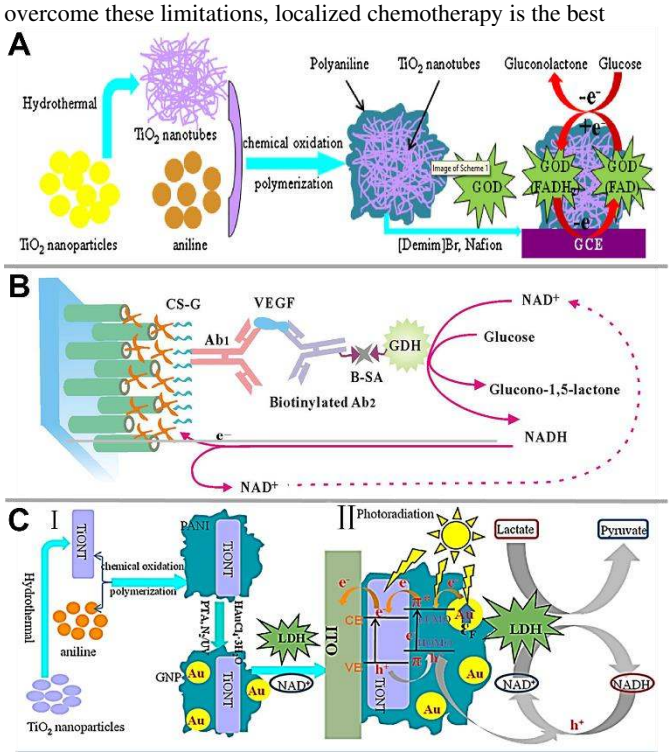

Fig. 14 (A) Fabrication process of the PANI–TNTs modified biosensor and the reaction scheme for catalytic oxidation of glucose under nitrogen atmosphere on it. Adapted with permission from ref. 233. Copyright 2015 Elsevier. (B) Schematic diagram of the immunoanalysis principle using the novel BiOI/TiO_2 NTs arrayed p-n junction photoelectrode. Adapted with permission from ref. 257. Copyright 2014 Springer Nature. (C) Schematic illustration for preparation of TNT-PANI-GNP ternary composite (I) and SPR-enhanced PEC detection of lactate at TNT-PANIGNP|LDH|NAD+|ITO coupling with PEC coenzyme regeneration (II). Adapted with permission from ref. 261. Copyright 2015 American Chemical Society.

Kaur *et al.* demonstrated a significant reduction in cancer cell viability under culture with TRAIL modified Ti-TNT implants (TRAIL-TNTs). TRAIL-TNTs exhibited an obvious regression in tumor burden within the first three days of implant insertion at the tumor site. Based on current experimental findings these Ti-TNTs implants have shown promising capacity to load and deliver anti-cancer agents maintaining their efficacy for cancer treatment.[264] It is possible to develop a more effective treatment for tumors by chemically loading the antineoplastic drug on the TNTs. Gulati *et al.* introduced a novel method to treat brain diseases based on drug-releasing TNTs implant.[265] The result indicated that anticancer drugs loaded TNTs exhibited controlled drug release *in vivo*, which could effectively kill cancer cells with an outstanding capacity for localized treatment. In conclusion, TNTs have great potential application in localized cancer therapy, and more advanced systems are expected to be designed for exploring these concepts in the future.

7. Conclusions and future perspectives

TNTs have become the most widely applied biomaterials for implant devices because of their excellent biocompatibility, corrosion resistance and mechanical property. This review summarizes recent research progress of TNTs in biomedical applications. TNTs exhibit a unique combination of biocompatibility and surface functionalization ability. Due to the excellent biocompatibility and controllable nanotube dimension and crystal structure, TNTs possess multiple meaningful functions, such as regulating protein adsorption, bacteria adhesion, platelet behavior and cellular interaction, inducing hydroxyapatite formation, and promoting osseointegration and hemocompatibility. TNTs could be functionalized with various biomolecules, or loaded with growth factors, antibiotics, anticoagulants and therapeutic metal NPs for special biomedical applications. Considerable *in vitro* and *in vivo* studies suggest that TNTs are a promising material for biomedical applications. Furthermore, surface modification of TNTs applied in titanium based orthopedic, dental and stent implants has little influence on the products appearance. The further development of TNTs still faces with many urgent challenges. Establishing a relationship between synthesis conditions and the nanostructure morphology of nanotubes is at all imminent. Considering that all implanted biomaterials are exposed to the danger of immunization, infection, thrombosis and fibrosis, which will potentially result in implant failure, improving the proper biointegration is expected to be a primary focus of the future titania-based biomedical researches.

Acknowledgements:

The authors thank the National Natural Science Foundation of China (21501127 and 51502185), and Jiangsu Advanced Textile Engineering Center Project (Project No. SPPGO[2014] 22). We also

acknowledge funds from the Priority Academic Program Development of Jiangsu Higher Education Institutions (PAPD) and the Project for Jiangsu Scientific and Technological Innovation Team (2013).

Reference:

1. G. Pfaff and P. Reynders, *Chem. Rev.*, 1999, **99**, 1963-1981.
2. A. B. a. R. E. M. Juergen H. Braun, *Prog. Org. Coat.*, 1992, **20**, 105-138.
3. S. Yuan, W. Chen and S. Hu, *Mater. Sci. Eng. C*, 2005, **25**, 479-485.
4. A. Fujishima and K. Honda, *Nature*, 1972, **238**, 37-38.
5. X.-Y. Zhang, H.-P. Li, X.-L. Cui and Y. Lin, *J. Mater. Chem.*, 2010, **20**, 2801-2806.
6. W.-T. Sun, Y. Yu, H.-Y. Pan, X.-F. Gao, Q. Chen and L.-M. Peng, *J. Am. Chem. Soc.*, 2008, **130**, 1124-1125.
7. J. R. Jennings, A. Ghicov, L. M. Peter, P. Schmuki and A. B. Walker, *J. Am. Chem. Soc.*, 2008, **130**, 13364-13372.
8. M. Geetha, A. K. Singh, R. Asokamani and A. K. Gogia, *Prog. Mater. Sci.*, 2009, **54**, 397-425.
9. S. Minagar, C. C. Berndt, J. Wang, E. Ivanova and C. Wen, *Acta Biomater.*, 2012, **8**, 2875-2888.
10. T. Kokubo, H.-M. Kim and M. Kawashita, *Biomaterials*, 2003, **24**, 2161-2175.
11. M. Navarro, A. Michiardi, O. Castano and J. A. Planell, *J. R. Soc. Interfaces*, 2008, **5**, 1137-1158.
12. J. Park, S. Bauer, K. A. Schlegel, F. W. Neukam, K. von der Mark and P. Schmuki, *Small*, 2009, **5**, 666-671.
13. S. Oh, C. Daraio, L. H. Chen, T. R. Pisanic, R. R. Finones and S. Jin, *J. Biomed. Mater. Res A*, 2006, **78**, 97-103.
14. Y. Lai, L. Lin, F. Pan, J. Huang, R. Song, Y. Huang, C. Lin, H. Fuchs and L. Chi, *Small*, 2013, **9**, 2945-2953.
15. Y. Xia, P. Yang, Y. Sun, Y. Wu, B. Mayers, B. Gates, Y. Yin, F. Kim and H. Yan, *Adv. Mater.*, 2003, **15**, 353-389.
16. K.-J. Hwang, D. W. Cho, J.-W. Lee and C. Im, *New J. Chem.*, 2012, **36**, 2094.
17. D. Wang, L. Zhang, W. Lee, M. Knez and L. Liu, *Small*, 2013, **9**, 1025-1029.
18. A. M. Md Jani, D. Losic and N. H. Voelcker, *Prog. Mater. Sci.*, 2013, **58**, 636-704.
19. C. Bae, H. Yoo, S. Kim, K. Lee, J. Kim, M. M. Sung and H. Shin, *Chem. Mater.*, 2008, **20**, 756-767.
20. P. Hoyer, *Adv. Mater.*, 1996, **8**, 857-859.
21. L. Yuan, S. Meng, Y. Zhou and Z. Yue, *J. Mater. Chem. A*, 2013, **1**, 2552-2557.
22. K. Huo, B. Gao, J. Fu, L. Zhao and P. K. Chu, *RSC Adv.*, 2014, **4**, 17300-17324.
23. M. Assefpour-Dezfuly, C. Vlachos and E. H. Andrews, *J. Mater. Sci. Mater. Med.*, 1984, **19**, 3626-3639.
24. D. Gong, C. A. Grimes and O. K. Varghese, *J. Mater. Res.*, 2001, **16**, 3331-3334.
25. Y. Lai, X. Gao, H. Zhuang, J. Huang, C. Lin and L. Jiang, *Adv.Mater.*, 2009, **21**, 3799-3803.
26. K. Shankar, G. K. Mor, H. E. Prakasam, S. Yoriya, M. Paulose, O. K. Varghese and C. A. Grimes, *Nanotechnology*, 2007, **18**, 065707.
27. S. Yoriya and C. A. Grimes, *Langmuir,* 2010, **26**, 417-420.
28. D. Yu, X. Zhu, Z. Xu, X. Zhong, Q. Gui, Y. Song, S. Zhang, X. Chen and D. Li, *ACS Appl. Mater. Interfaces*, 2014, **6**, 8001-8005.
29. M. Z. Ge, Q. S. Li, C. Y. Cao, J. Y. Huang, S. H. Li, S. N. Zhang, Z. Chen, K. Q. Zhang, S. S. Al-Deyab and Y. K. Lai, *Adv. Sci.*, 2017, **4**, 1600152.
30. T. Kasuga, M. Hiramatsu, A. Hoson, T. Sekino and K. Niihara, *Adv. Mater.*, 1999, **11**, 1307-1311.
31. P. Roy, S. Berger and P. Schmuki, *Angew. Chem. Int. Ed.*, 2011, **50**, 2904-2939.
32. P. Hoyer, *Langmuir*, 1996, **12**, 1411-1413.
33. D. V. Bavykin, J. M. Friedrich and F. C. Walsh, *Adv. Mater.*, 2006, **18**, 2807-2824.
34. C.-C. Tsai and H. Teng, *Chem. Mater.*, 2006, **18**, 367-373.
35. P. Liu, H. Zhang, H. Liu, Y. Wang, X. Yao, G. Zhu, S. Zhang and H. Zhao, *J. Am. Chem. Soc.*, 2011, **133**, 19032-19035.
36. A. Kukovecz, N. Hodos, E. Horvath, G. Radnoczi, Z. Konya and I. Kiricsi, *J. Phys. Chem. B*, 2005, **109**, 17781-17783.
37. B. Poudel, W. Z. Wang, C. Dames, J. Y. Huang, S. Kunwar, D. Z. Wang, D. Banerjee, G. Chen and Z. F. Ren, *Nanotechnology*, 2005, **16**, 1935-1940.
38. Z. V. Saponjic, N. M. Dimitrijevic, D. M. Tiede, A. J. Goshe, X. Zuo, L. X. Chen, A. S. Barnard, P. Zapol, L. Curtiss and T. Rajh, *Adv. Mater.*, 2005, **17**, 965-971.
39. Z.-Y. Yuan and B.-L. Su, *Colloids Surf. A*, 2004, **241**, 173-183.
40. A. L, Linsebigler, G. Lu, J. T. and J. Yates, *Chem. Rev.*, 1995, **95**, 735-758.
41. U. Diebold, *Surf. Sci. Rep.*, 2003, **48**, 53-229.
42. A. Fujishima, X. Zhang and D. Tryk, *Surf. Sci. Rep.*, 2008, **63**, 515-582.
43. A. Kubacka, M. Fernandez-Garcia and G. Colon, *Chem. Rev.*, 2012, **112**, 1555-1614.
44. S. Chen, Y. Zhu, W. Li, W. Liu, L. Li, Z. Yang, C. Liu, W. Yao, X. Lu and X. Feng, *Chinese J. Catal.*, 2010, **31**, 605-614.
45. Q. Tay, X. Liu, Y. Tang, Z. Jiang, T. C. Sum and Z. Chen, *J. Phys. Chem. C*, 2013, **117**, 14973-14982.
46. H. Zhang and J. F. Banfield, *J. Phys. Chem. B*, 2000, **104**, 3481-3487.
47. T. L. Thompson and J. T. Yates, *Chem. Rev.*, 2006, **106**, 4428-4453.
48. S. Beke, R. Barenghi, B. Farkas, I. Romano, L. Korosi, S. Scaglione and F. Brandi, *Mater. Sci. Eng. C*, 2014, **44**, 38-43.
49. W. Q. Yu, J. Qiu and F. Q. Zhang, *Colloids Surf. B*, 2011, **84**, 400-405.
50. A. Majeed, J. He, L. R. Jiao, X. X. Zhong and Z. M. Sheng, *Nanoscale Res. Lett.*, 2015, **10**, 1-9.
51. W. L. Lu, N. Wang, P. Gao, C. Y. Li, H. S. Zhao and Z. T. Zhang, *Cell Proliferat.*, 2015, **48**, 95-104.
52. Y. Li, F. Li, C. Zhang, B. Gao, P. Tan, B. Mi, Y. Zhang, H. Cheng, H. Liao, K. Huo and W. Xiong, *J. Nanosci. Nanotechnol.*, 2015, **15**, 4136-4142.
53. C. X. Shan, X. Hou and K.-L. Choy, *Surf. Coat. Tech.*, 2008, **202**, 2399-2402.

54. Y. Fovet, J. Y. Gal and F. Toumelin-Chemla, *Talanta*, 2001, **53**, 1053-1063.
55. C. Grosso, P. Valentao, F. Ferreres and P. B. Andrade, *Mar. Drugs*, 2014, **12**, 2539-2589.
56. M. M. Gentleman and E. Gentleman, *Int. Mater. Rev.*, 2014, **59**, 417-429.
57. W. Peng, Z. Qiao, Q. Zhang, X. Cao, X. Chen, H. Dong, J. Liao and C. Ning, *J. Mater. Chem. B*, 2013, **1**, 3506-3512.
58. M. Kulkarni, A. Mazare, J. Park, E. Gongadze, M. S. Killian, S. Kralj, K. von der Mark, A. Iglic and P. Schmuki, *Acta Biomater.*, 2016, **45**, 357-366.
59. M. Kulkarni, A. Flasker, M. Lokar, K. Mrak-Poljsak, A. Mazare, A. Artenjak, S. Cucnik, S. Kralj, A. Velikonja, P. Schmuki, V. Kralj-Iglic, S. Sodin-Semrl and A. Iglic, *Int. J. Nanomed.*, 2015, **10**, 1359-1373.
60. E. Gongadze, D. Kabaso, S. Bauer, T. Slivnik, P. Schmuki, U. van Rienen and A. Iglic, *Int. J. Nanomed.*, 2011, **6**, 1801-1816.
61. S. C. Roy, M. Paulose and C. A. Grimes, *Biomaterials*, 2007, **28**, 4667-4672.
62. B. S. Kopf, A. Schipanski, M. Rottmar, S. Berner and K. Maniura-Weber, *Acta Biomater.*, 2015, **19**, 180-190.
63. B. S. Smith and K. C. Popat, *J. Biomed. Nanotechnol.*, 2012, **8**, 642-658.
64. B. S. Smith, S. Yoriya, L. Grissom, C. A. Grimes and K. C. Popat, *J. Biomed. Mater. Res. A*, 2010, **95**, 350-360.
65. L. Zhang, X. Liao, A. Fok, C. Ning, P. Ng and Y. Wang, *Mater. Sci. Eng. C*, 2018, **82**, 91-101.
66. Q. Huang, Y. Yang, D. Zheng, R. Song, Y. Zhang, P. Jiang, E. A. Vogler and C. Lin, *Acta Biomater.*, 2017, **51**, 505-512.
67. Y. Yang, Y. Lai, Q. Zhang, K. Wu, L. Zhang, C. Lin and P. Tang, *Colloids Surf. B*, 2010, **79**, 309-313.
68. M. Rai, A. Yadav and A. Gade, *Biotechnol. Adv.*, 2009, **27**, 76-83.
69. E. P. Ivanova, V. K. Truong, J. Y. Wang, C. C. Berndt, R. T. Jones, Yusuf, II, I. Peake, H. W. Schmidt, C. Fluke, D. Barnes and R. J. Crawford, *Langmuir*, 2010, **26**, 1973-1982.
70. S. D. Puckett, E. Taylor, T. Raimondo and T. J. Webster, *Biomaterials*, 2010, **31**, 706-713.
71. N. Abbas, G. N. Shao, M. S. Haider, S. M. Imran, S. S. Park, S. J. Jeon and H. T. Kim, *Mater. Sci. Eng. C*, 2016, **68**, 780-788.
72. S. Li, T. Zhu, J. Huang, Q. Guo, G. Chen and Y. Lai, *Int. J. Nanomed.*, 2017, **12**, 2593-2606.
73. B. Ercan, E. Taylor, E. Alpaslan and T. J. Webster, *Nanotechnology*, 2011, **22**, 295102.
74. K. Narendrakumar, M. Kulkarni, O. Addison, A. Mazare, I. Junkar, P. Schmuki, R. Sammons and A. Iglic, *Dent. Mater.*, 2015, **31**, 1460-1468.
75. K. M. Kummer, E. N. Taylor, N. G. Durmas, K. M. Tarquinio, B. Ercan and T. J. Webster, *J. Biomed. Mater. Res. B*, 2013, **101**, 677-688.
76. H. Li, Q. Cui, B. Feng, J. Wang, X. Lu and J. Weng, *Appl. Surf. Sci.*, 2013, **284**, 179-183.
77. L. Zhang, L. Zhang, Y. Yang, W. Zhang, H. Lv, F. Yang, C. Lin and P. Tang, *J. Biomed. Mater. Res. B*, 2016, **104**, 1004-1012.
78. A. W. Tan, B. Pingguan-Murphy, R. Ahmad and S. A. Akbar, *Ceram. Int.*, 2012, **38**, 4421-4435.
79. R. Song, J. H. Liang, L. X. Lin, Y. M. Zhang, Y. Yang and C. J. Lin, *J. Mater. Chem. B*, 2016, **4**, 4017-4024.
80. B. Feng, J. Weng, B. C. Yang, S. X. Qu and X. D. Zhang, *Biomaterials*, 2003, **24**, 4663-4670.
81. W. Q. Yu, X. Q. Jiang, F. Q. Zhang and L. Xu, *J. Biomed. Mater. Res. A*, 2010, **94**, 1012-1022.
82. N. Wang, H. Li, W. Lu, J. Li, J. Wang, Z. Zhang and Y. Liu, *Biomaterials*, 2011, **32**, 6900-6911.
83. K. S. Brammer, S. Oh, J. O. Gallagher and S. Jin, *Nano Lett.*, 2008, **8**, 786-793.
84. L. Liu, R. Bhatia and T. J. Webster, *Int. J. Nanomed.*, 2017, **12**, 8711-8723.
85. S. Minagar, Y. Li, C. C. Berndt and C. Wen, *Acta Biomater.*, 2015, **12**, 281-289.
86. C. V. Wilmowsky, S. Bauer, S. Roedl, F. W. Neukam, P. Schmuki and K. A. Schlegel, *Clin. Oral. Implan. Res.*, 2012, **23**, 359-366.
87. K. S. Brammer, S. Oh, C. J. Frandsen, S. Varghese and S. Jin, *Mater. Sci. Eng. C*, 2010, **30**, 518-525.
88. A. Mazare, M. Dilea, D. Ionita, I. Titorencu, V. Trusca and E. Vasile, *Bioelectrochemistry*, 2012, **87**, 124-131.
89. W. Q. Yu, Y. L. Zhang, X. Q. Jiang and F. Q. Zhang, *Oral. Dis.*, 2010, **16**, 624-630.
90. S.-H. An, R. Narayanan, T. Matsumoto, H.-J. Lee, T.-Y. Kwon and K.-H. Kim, *J. Nanosci. Nanotechnol.*, 2011, **11**, 4910-4918.
91. J. Park, S. Bauer, K. V. d. Mark and P. Schmuki, *Nano Lett.*, 2007, **7**, 1686-1691.
92. H. Y. Seo, J. S. Kwon, Y. R. Choi, K. M. Kim, E. H. Choi and K. N. Kim, *Plos One*, 2014, **9**, e113477.
93. M. Mansoorianfar, M. Tavoosi, R. Mozafarinia, A. Ghasemi and A. Doostmohammadi, *Surf. Coat. Tech.*, 2017, **321**, 409-415.
94. M. D. Heath, B. Henderson and S. Perkin, *Langmuir*, 2010, **26**, 5304-5308.
95. J. Wang, Y. An, F. Li, D. Li, D. Jing, T. Guo, E. Luo and C. Ma, *Acta Biomater.*, 2014, **10**, 975-985.
96. M. Kulkarni, A. Mazare, E. Gongadze, S. Perutkova, V. Kralj-Iglic, I. Milosev, P. Schmuki, A. Iglic and M. Mozetic, *Nanotechnology*, 2015, **26**, 062002.
97. C. J. Wilson, R. E. Clegg, D. I. Leavesley and M. J. Pearcy, *Tissue Eng.*, 2005, **11**, 1-18.
98. S. Bauer, J. Park, K. von der Mark and P. Schmuki, *Acta Biomater.*, 2008, **4**, 1576-1582.
99. Y. Lai, F. Pan, C. Xu, H. Fuchs and L. Chi, *Adv. Mater.*, 2013, **25**, 1682-1686.
100. Y. Lai, Y. Huang, H. Wang, J. Huang, Z. Chen and C. Lin, *Colloids Surf. B*, 2010, **76**, 117-122.
101. J. Y. Huang, Y. K. Lai, F. Pan, L. Yang, H. Wang, K. Q. Zhang, H. Fuchs and L. F. Chi, *Small*, 2014, **10**, 4865-4873.
102. H. Li, Y. Lai, J. Huang, Y. Tang, L. Yang, Z. Chen, K. Zhang, X. Wang and L. P. Tan, *J. Mater. Chem. B*, 2015, **3**, 342-347.
103. L. Zhao, S. Mei, W. Wang, P. K. Chu, Z. Wu and Y. Zhang, *Biomaterials*, 2010, **31**, 2055-2063.
104. K. S. Brammer, C. J. Frandsen and S. Jin, *Trends*

Biotechnol., 2012, **30**, 315-322.
105. Q. L. Ma, L. Z. Zhao, R. R. Liu, B. Q. Jin, W. Song, Y. Wang, Y. S. Zhang, L. H. Chen and Y. M. Zhang, *Biomaterials*, 2014, **35**, 9853-9867.
106. L. Xia, B. Feng, P. Wang, S. Ding, Z. Liu, J. Zhou and R. Yu, *Int. J. Nanomed.*, 2012, **7**, 4873-4881.
107. X. Shen, P. Ma, Y. Hu, G. Xu, K. Xu, W. Chen, Q. Ran, L. Dai, Y. Yu, C. Mu and K. Cai, *J. Mater. Chem. B*, 2016, **4**, 1423-1436.
108. L. Bai, R. Wu, Y. Wang, X. Wang, X. Zhang, X. Huang, L. Qin, R. Hang, L. Zhao and B. Tang, *J. Mater. Chem. B*, 2016, **4**, 5548-5559.
109. H.-L. Huang, Y.-Y. Chang, M.-C. Lai, C.-R. Lin, C.-H. Lai and T.-M. Shieh, *Surf. Coat. Tech.*, 2010, **205**, 1636-1641.
110. S. Moosavi Nejad, H. Takahashi, H. Hosseini, A. Watanabe, H. Endo, K. Narihira, T. Kikuta and K. Tachibana, *Ultrason. Sonochem.*, 2016, **32**, 95-101.
111. R. Z. Legeros and R. G. Craig, *J. Bone Miner. Res.*, 1993, **8**, S583-S596.
112. S. Nayak, T. Dey, D. Naskar and S. C. Kundu, *Biomaterials*, 2013, **34**, 2855-2864.
113. W. F. Oliveira, I. R. S. Arruda, G. M. M. Silva, G. Machado, L. Coelho and M. T. S. Correia, *Mater. Sci. Eng. C*, 2017, **81**, 597-606.
114. F. Mirri, A. K. Ma, N. B. Tienyi T. Hsu, S. L. Eichmann, C. C. Young, D. E. Tsentalovich and M. Pasquali, *ACS Nano*, 2012, **6**, 9737–9744.
115. M. Lai, K. Cai, L. Zhao, X. Chen, Y. Hou and Z. Yang, *Biomacromolecules*, 2011, **12**, 1097-1105.
116. H. Wei, S. Wu, Z. Feng, W. Zhou, Y. Dong, G. Wu, S. Bai and Y. Zhao, *Int. J. Nanomed.*, 2012, **7**, 1091-1100.
117. S. Dastgheyb, J. Parvizi, I. M. Shapiro, N. J. Hickok and M. Otto, *J. Infect. Dis.*, 2015, **211**, 641-650.
118. Y. Hu, K. Cai, Z. Luo, D. Xu, D. Xie, Y. Huang, W. Yang and P. Liu, *Acta Biomater.*, 2012, **8**, 439-448.
119. K. Gulati, S. Ramakrishnan, M. S. Aw, G. J. Atkins, D. M. Findlay and D. Losic, *Acta Biomater.*, 2012, **8**, 449-456.
120. X. Chen, K. Cai, J. Fang, M. Lai, Y. Hou, J. Li, Z. Luo, Y. Hu and L. Tang, *Colloids Surf. B*, 2013, **103**, 149-157.
121. H. Wang, L. Wei, Z. Wang and S. Chen, *RSC Adv.*, 2016, **6**, 14097-14104.
122. Y. Yang, X. Li, H. Qiu, P. Li, P. Qi, M. F. Maitz, T. You, R. Shen, Z. Yang, W. Tian and N. Huang, *ACS Appl. Mater. Interfaces*, 2017.
123. D. T. Sponza and R. Oztekin, *Desalin. Water Treat.*, 2017, **71**, 116-135.
124. M. R. Mohammadi, D. J. Fray and M. C. Cordero-Cabrera, *Sens. Actuators B Chem.*, 2007, **124**, 74-83.
125. Y. Hu, Z. Gao, W. Sun and X. Liu, *Colloids Surf. A*, 2012, **415**, 439-448.
126. M. P. Neupane, I. S. Park, T. S. Bae, H. K. Yi, M. Uo, F. Watari and M. H. Lee, *J. Mater. Chem.*, 2011, **21**, 12078-12082.
127. M. Lai, Z. Jin, X. Yang, H. Wang and K. Xu, *Appl. Surf. Sci.*, 2017, **396**, 1741-1751.
128. A. K. M. Kafi, G. Wu, P. Benvenuto and A. Chen, *J. Electroanal. Chem.*, 2011, **662**, 64-69.
129. H. C. Lee, L. F. Zhang, J. L. Lin, Y. L. Chin and T. P. Sun, *Sensors*, 2013, **13**, 14161-14174.
130. P. Benvenuto, A. K. M. Kafi and A. Chen, *J. Electroanal. Chem.*, 2009, **627**, 76-81.
131. Z. D. Gao, Y. Qu, T. Li, N. K. Shrestha and Y. Y. Song, *Sci. Rep.*, 2014, **4**, 6891.
132. Z. Shi, G. Xueping, S. Deying, Y. Zhou and D. Yan, *Polymer*, 2007, **48**, 7516-7522.
133. M. Kazemzadeh-Narbat, B. F. Lai, C. Ding, J. N. Kizhakkedathu, R. E. Hancock and R. Wang, *Biomaterials*, 2013, **34**, 5969-5977.
134. M. Ma, M. Kazemzadeh-Narbat, Y. Hui, S. Lu, C. Ding, D. D. Chen, R. E. Hancock and R. Wang, *J. Biomed. Mater. Res. A*, 2012, **100**, 278-285.
135. M. Lai, Z. Jin and Z. Su, *Mater. Sci. Eng. C*, 2017, **73**, 490-497.
136. G.-H. Kim, l.-S. Kim, S.-W. Park, K. Lee, K.-D. Yun, H.-S. Kim, G.-J. Oh, M.-K. Ji and H.-P. Lim, *J. Nanosci. Nanotechnol.*, 2016, **16**, 1396-1399.
137. X. Cao, W. Q. Yu, J. Qiu, Y. F. Zhao, Y. L. Zhang and F. Q. Zhang, *J. Mater. Sci. Mater. Med.*, 2012, **23**, 527-536.
138. D. P. Song, M. J. Chen, Y. C. Liang, Q. S. Bai, J. X. Chen and X. F. Zheng, *Acta Biomater.*, 2010, **6**, 684-694.
139. S. Sun, W. Yu, Y. Zhang and F. Zhang, *J. Mater. Sci. Mater. Med.*, 2013, **24**, 1079-1091.
140. S. Bauer, J. Park, A. Pittrof, Y. Y. Song, K. von der Mark and P. Schmuki, *Integr. Biol.*, 2011, **3**, 927-936.
141. X. Chen, J. Zhao, A. Li, P. Gao, J. Sun, Y. Song, J. Liu, P. Chen and Z. Wang, *Onco Targets Ther*, 2016, **9**, 3205-3212.
142. N. K. Awad, S. L. Edwards and Y. S. Morsi, *Mater. Sci. Eng. C*, 2017, **76**, 1401-1412.
143. Y. Yang, Y. Zhang, R. Hu, Q. Huang, K. Wu, L. Zhang, P. Tang and C. Lin, *RSC Adv.*, 2017, **7**, 38434-38443.
144. C. Zhao, B. Feng, Y. Li, J. Tan, X. Lu and J. Weng, *Appl. Surf. Sci.*, 2013, **280**, 8-14.
145. Z. Jia, P. Xiu, M. Li, X. Xu, Y. Shi, Y. Cheng, S. Wei, Y. Zheng, T. Xi, H. Cai and Z. Liu, *Biomaterials*, 2016, **75**, 203-222.
146. L. Zhao, H. Wang, K. Huo, L. Cui, W. Zhang, H. Ni, Y. Zhang, Z. Wu and P. K. Chu, *Biomaterials*, 2011, **32**, 5706-5716.
147. H. Qin, H. Cao, Y. Zhao, C. Zhu, T. Cheng, Q. Wang, X. Peng, M. Cheng, J. Wang, G. Jin, Y. Jiang, X. Zhang, X. Liu and P. K. Chu, *Biomaterials*, 2014, **35**, 9114-9125.
148. M. Li, Q. Liu, Z. Jia, X. Xu, Y. Shi, Y. Cheng and Y. Zheng, *J. Mater. Chem. B*, 2015, **3**, 8796-8805.
149. Z. D. Gao, H. F. Liu, C. Y. Li and Y. Y. Song, *Chem. Commun.*, 2013, **49**, 774-776.
150. J. Xu, X. Zhou, Z. Gao, Y. Y. Song and P. Schmuki, *Angew. Chem. Int. Ed.*, 2016, **55**, 593-597.
151. K. Huo, X. Zhang, H. Wang, L. Zhao, X. Liu and P. K. Chu, *Biomaterials*, 2013, **34**, 3467-3478.
152. W. Liu, P. Su, A. Gonzales, 3rd, S. Chen, N. Wang, J. Wang, H. Li, Z. Zhang and T. J. Webster, *Int. J. Nanomed.*, 2015, **10**, 1997-2019.
153. V. S. Voruganti, G. L. Klein, H. X. Lu, S. Thomas, J. H. Freeland-Graves and D. N. Herndon, *Burns*, 2005, **31**, 711-

716.
154. Y. Qin, C. Zhu, J. Chen, D. Liang and G. Wo, *J. Appl. Polym. Sci.*, 2007, **105**, 527-532.
155. J. Rosenbaum, D. L. Versace, S. Abbad-Andallousi, R. Pires, C. Azevedo, P. Cenedese and P. Dubot, *Biomater. Sci.*, 2017, **5**, 455-462.
156. G. Jin, H. Qin, H. Cao, Y. Qiao, Y. Zhao, X. Peng, X. Zhang, X. Liu and P. K. Chu, *Biomaterials*, 2015, **65**, 22-31.
157. Y. Zhao, H. Cao, H. Qin, T. Cheng, S. Qian, M. Cheng, X. Peng, J. Wang, Y. Zhang, G. Jin, X. Zhang, X. Liu and P. K. Chu, *ACS Appl. Mater. Interfaces*, 2015, **7**, 17826-17836.
158. D. Y. Kim, M. Kim, H. E. Kim, Y. H. Koh, H. W. Kim and J. H. Jang, *Acta Biomater.*, 2009, **5**, 2196-2205.
159. Y. Liu, S. Kim, J. A. McLeod, J. Li, X. X. Guo, T. K. Sham and L. J. Liu, *Appl. Surf. Sci.*, 2017, **396**, 1212-1219.
160. D. Ionita, D. Bajenaru-Georgescu, G. Totea, A. Mazare, P. Schmuki and I. Demetrescu, *Int. J. Pharm.*, 2017, **517**, 296-302.
161. B. Feng, X. Chu, J. Chen, J. Wang, X. Lu and J. Weng, *J. Porous Mater.*, 2009, **17**, 453-458.
162. A. Kar, K. S. Raja and M. Misra, *Surf. Coat. Tech.*, 2006, **201**, 3723-3731.
163. S. Eraković, A. Janković, C. Ristoscu, L. Duta, N. Serban, A. Visan, I. N. Mihailescu, G. E. Stan, M. Socol, O. Iordache, I. Dumitrescu, C. R. Luculescu, D. Janaćković and V. Mišković-Stanković, *Appl. Surf. Sci.*, 2014, **293**, 37-45.
164. X. Lu, H. Zhang, Y. Guo, Y. Wang, X. Ge, Y. Leng and F. Watari, *CrystEngComm*, 2011, **13**, 3741-3749.
165. K. C. Popat, M. Eltgroth, T. J. LaTempa, C. A. Grimes and T. A. Desai, *Small*, 2007, **3**, 1878-1881.
166. N. Khoshnood, A. Zamanian and A. Massoudi, *Mater. Sci. Eng. C*, 2017, **77**, 748-754.
167. M. S. Aw, K. A. Khalid, K. Gulati, G. J. Atkins, P. Pivonka, D. M. Findlay and D. Losic, *Int. J. Nanomed.*, 2012, **7**, 4883-4892.
168. Q. Wang, J. Y. Huang, H. Q. Li, A. Z. Zhao, Y. Wang, K. Q. Zhang, H. T. Sun and Y. K. Lai, *Int. J. Nanomed.*, 2017, **12**, 151-165.
169. C. Xu, Z. Wei, H. Gao, Y. Bai, H. Liu, H. Yang, Y. Lai and L. Yang, *Adv. Sci.*, 2017, **4**, 1600410.
170. Y. Dong, H. Ye, Y. Liu, L. Xu, Z. Wu, X. Hu, J. Ma, J. L. Pathak, J. Liu and G. Wu, *Colloids Surf. A*, 2017, **158**, 127-136.
171. K. Gulati, M. Kogawa, M. Prideaux, D. M. Findlay, G. J. Atkins and D. Losic, *Mater. Sci. Eng. C*, 2016, **69**, 831-840.
172. L. L. Peng, A. D. Mendelsohn, T. J. LaTempa, S. Yoriya, C. A. Grimes and T. A. Desai, *Nano Lett.*, 2009, **9**, 1932-1936.
173. K. C. Popat, M. Eltgroth, T. J. Latempa, C. A. Grimes and T. A. Desai, *Biomaterials*, 2007, **28**, 4880-4888.
174. K. Gulati and S. Ivanovski, *Expert Opin. Drug Deliv.*, 2017, **14**, 1009-1024.
175. M. S. Aw, J. Addai-Mensah and D. Losic, *Chem. Commun.*, 2012, **48**, 3348-3350.
176. Q. Wang, J. Y. Huang, H. Q. Li, Z. Chen, A. Z. Zhao, Y. Wang, K. Q. Zhang, H. T. Sun, S. S. Al-Deyab and Y. K. Lai, *Int. J. Nanomed.*, 2016, **11**, 4819-4834.
177. P. Huang, J. Wang, S. Lai, F. Liu, N. Ni, Q. Cao, W. Liu, D. Y. B. Deng and W. Zhou, *J. Mater. Chem. B*, 2014, **2**, 8616-8625.
178. M. E. Barbinta-Patrascu, C. Ungureanu, S. M. Iordache, I. R. Bunghez, N. Badea and I. Rau, *J. Mater. Chem. B*, 2014, **2**, 3221-3231.
179. C. J. Hedegaard, M. L. Strube, M. B. Hansen, B. K. Lindved, A. Lihme, M. Boye and P. M. Heegaard, *Plos One*, 2016, **11**, e0147373.
180. S. Popescu, C. Ungureanu, A. M. Albu and C. Pirvu, *Prog. Org. Coat.*, 2014, **77**, 1890-1900.
181. G. I. Frengova and D. M. Beshkova, *J. Ind. Microbiol. Biotechnol.*, 2009, **36**, 163-180.
182. R. P. Allaker and K. Memarzadeh, *Int. J. Antimicrob. Agents*, 2014, **43**, 95-104.
183. T. J. Vaughan, C. T. McCarthy and L. M. McNamara, *J. Mech. Behav. Biomed. Mater.*, 2012, **12**, 50-62.
184. A. Arsiwala, P. Desai and V. Patravale, *J. Control. Release*, 2014, **189**, 25-45.
185. F. Nasirpouri, I. Yousefi, E. Moslehifard and J. Khalil-Allafi, *Surf. Coat. Tech.*, 2017, **315**, 163-171.
186. D. Khudhair, H. Amani Hamedani, J. Gaburro, S. Shafei, S. Nahavandi, H. Garmestani and A. Bhatti, *Mater. Sci. Eng. C*, 2017, **77**, 111-120.
187. R. Kralchevska, M. Milanova, D. Hristov, A. Pintar and D. Todorovsky, *Mater. Res. Bull.*, 2012, **47**, 2165-2177.
188. F. Hilario, V. Roche, R. P. Nogueira and A. M. J. Junior, *Electrochim. Acta*, 2017, **245**, 337-349.
189. M. S. Lord, M. Foss and F. Besenbacher, *Nano Today*, 2010, **5**, 66-78.
190. Y. Sugita, K. Ishizaki, F. Iwasa, T. Ueno, H. Minamikawa, M. Yamada, T. Suzuki and T. Ogawa, *Biomaterials*, 2011, **32**, 8374-8384.
191. C. Mas-Moruno, B. Garrido, D. Rodriguez, E. Ruperez and F. J. Gil, *J. Mater. Sci. Mater. Med.*, 2015, **26**, 109.
192. I. S. Park, E. J. Yang and T. S. Bae, *Biomed Res Int*, 2013, **2013**, 293627.
193. A. M. Arsiwala, A. J. Raval and V. B. Patravale, *Pharm. Pat. Analyst*, 2013, **2**, 499-512.
194. H. Cheng, W. Xiong, Z. Fang, H. Guan, W. Wu, Y. Li, Y. Zhang, M. M. Alvarez, B. Gao, K. Huo, J. Xu, N. Xu, C. Zhang, J. Fu, A. Khademhosseini and F. Li, *Acta Biomater.*, 2016, **31**, 388-400.
195. X. Liu, Y. Zhang, S. Li, Y. Wang, T. Sun, Z. Li, L. Cai, X. Wang, L. Zhou and R. Lai, *Int. J. Nanomed.*, 2016, **11**, 6307-6324.
196. H. Shao, J. Shen, M. Wang, J. Cui, Y. Wang, S. Zhu, W. Zhang, H. Yang, Y. Xu and D. Geng, *Biomaterials*, 2015, **60**, 92-99.
197. E. S. Kim, E. J. Park and P. H. Choung, *J. Prosthet. Dent.*, 2001, **86**, 428-433.
198. T. L. Aghaloo, P. K. Moy and E. G. Freymiller, *J. Oral. Maxillofac. Surg.*, 2002, **60**, 1176-1181.
199. Y. Kozai, R. Kawamata, T. Sakurai, M. Kanno and I. Kashima, *Dentomaxillofac. Radiol.*, 2009, **38**, 34-41.
200. K. Donath, M. Laass and H. J. Gunzl, *Virchows Arch. A Pathol. Anat. Histopathol.*, 1992, **420**, 131-137.

201. S. B. Patel, N. Baker, I. Marques, A. Hamlekhan, M. T. Mathew, C. Takoudis, C. Friedrich, C. Sukotjo and T. Shokuhfar, *RSC Adv.*, 2017, **7**, 30397-30410.
202. G. E. Aninwene, C. Yao and T. J. Webster, *Int. J Nanomed.*, 2008, **3**, 257-264.
203. S. A. Alves, S. B. Patel, C. Sukotjo, M. T. Mathew, P. N. Filho, J.-P. Celis, L. A. Rocha and T. Shokuhfar, *Appl. Surf. Sci.*, 2017, **399**, 682-701.
204. B.-M. Seo, M. Miura, S. Gronthos, P. Mark Bartold, S. Batouli, J. Brahim, M. Young, P. Gehron Robey, C. Y. Wang and S. Shi, *Lancet*, 2004, **364**, 149-155.
205. H. Maeda, A. Tomokiyo, S. Fujii, N. Wada and A. Akamine, *Stem Cell Res. Ther.*, 2011, **2**, 33.
206. I. S. Song, Y. S. Han, J.-H. Lee, S. Um, H. Y. Kim and B. M. Seo, *Curr. Oral. Health Rep.*, 2015, **2**, 236-244.
207. Z. Li, J. Qiu, L. Q. Du, L. Jia, H. Liu and S. Ge, *Mater. Sci. Eng. C*, 2017, **76**, 684-691.
208. Y.-T. Sul, *Int. J. Nanomed.*, 2010, **5**, 87-100.
209. T. Monetta, A. Acquesta, A. Carangelo and F. Bellucci, *Metals*, 2017, **7**, 167.
210. I. Jang, S. C. Shim, D. S. Choi, B. K. Cha, J. K. Lee, B. H. Choe and W. Y. Choi, *Biomed. Microdevices*, 2015, **17**, 76.
211. I. Jang, D. S. Choi, J. K. Lee, W. T. Kim, B. K. Cha and W. Y. Choi, *Biomed. Microdevices*, 2017, **19**, 94.
212. P. A. Norowski, Jr. and J. D. Bumgardner, *J. Biomed. Mater. Res. B*, 2009, **88**, 530-543.
213. T. Kumeria, H. Mon, M. S. Aw, K. Gulati, A. Santos, H. J. Griesser and D. Losic, *Colloids Surf. B*, 2015, **130**, 255-263.
214. S. H. Nemati and A. Hadjizadeh, *AAPS PharmSciTech*, 2017, **18**, 2180-2187.
215. I. Chopra, *J. Antimicrob. Chemother.*, 2007, **59**, 587-590.
216. Q. Chang, L. Yan, M. Chen, H. He and J. Qu, *Langmuir*, 2007, **23**, 11197-11199.
217. D. Moretto, M. Gargari, E. Nordsjo, F. Gloria and L. Ottria, *Oral Implantol.*, 2008, **1**, 50-55.
218. G. I. Benic, D. S. Thoma, I. Sanz-Martin, F. Munoz, C. H. F. Hammerle, A. Cantalapiedra, J. Fischer and R. E. Jung, *Clin. Oral. Implants Res.*, 2017, **28**, 1592-1599.
219. S. Kotla, N. K. Singh, M. R. Heckle, G. J. Tigyi and G. N. Rao, *Sci. Signal.*, 2013, **6**, ra83.
220. P. Libby, P. M. Ridker and G. K. Hansson, *Nature*, 2011, **473**, 317-325.
221. A. I. Qureshi and L. R. Caplan, *The Lancet*, 2014, **383**, 984-998.
222. Y. Yang, P. Qi, F. Wen, X. Li, Q. Xia, M. F. Maitz, Z. Yang, R. Shen, Q. Tu and N. Huang, *ACS Appl. Mater. Interfaces*, 2014, **6**, 14608-14620.
223. E. M. Rzucidlo, K. A. Martin and R. J. Powell, *J. Vasc. Surg.*, 2007, **45**, A25-32.
224. L. Peng, M. L. Eltgroth, T. J. LaTempa, C. A. Grimes and T. A. Desai, *Biomaterials*, 2009, **30**, 1268-1272.
225. J. Li, K. Zhang, P. Yang, W. Qin, G. Li, A. Zhao and N. Huang, *Colloids Surf. A*, 2013, **110**, 199-207.
226. J. Li, K. Zhang, P. Yang, Y. Liao, L. Wu, J. Chen, A. Zhao, G. Li and N. Huang, *Exp. Cell Res.*, 2013, **319**, 2663-2672.
227. Z. Yang, S. Zhong, Y. Yang, M. F. Maitz, X. Li, Q. Tu, P. Qi, H. Zhang, H. Qiu, J. Wang and N. Huang, *J. Mater. Chem. B*, 2014, **2**, 6767-6778.
228. G. Chamberlain, J. Fox, B. Ashton and J. Middleton, *Stem Cells*, 2007, **25**, 2739-2749.
229. C. Vater, P. Kasten and M. Stiehler, *Acta Biomater.*, 2011, **7**, 463-477.
230. J. Li, W. Qin, K. Zhang, F. Wu, P. Yang, Z. He, A. Zhao and N. Huang, *Colloids Surf. B*, 2016, **145**, 410-419.
231. H. Nuhn, C. E. Blanco and T. A. Desai, *ACS Appl. Mater. Interfaces*, 2017, **9**, 19677-19686.
232. Y. B. Xie, L. M. Zhou and H. T. Huang, *Biosensors & bioelectronics*, 2007, **22**, 2812-2818.
233. J. Zhu, X. Liu, X. Wang, X. Huo and R. Yan, *Sens. Actuators B Chem.*, 2015, **221**, 450-457.
234. S. Park, H. Boo and T. D. Chung, *Anal. Chim. Acta*, 2006, **556**, 46-57.
235. Y.-Y. Song, Z. Gao, K. Lee and P. Schmuki, *Electrochem. Commun.*, 2011, **13**, 1217-1220.
236. Y. Wang, J. Chen, C. Zhou, L. Zhou, Y. Kong, H. Long and S. Zhong, *Electrochim. Acta*, 2014, **115**, 269-276.
237. S. Luo, F. Su, C. Liu, J. Li, R. Liu, Y. Xiao, Y. Li, X. Liu and Q. Cai, *Talanta*, 2011, **86**, 157-163.
238. X. Pang, D. He, S. Luo and Q. Cai, *Sens. Actuators B Chem.*, 2009, **137**, 134-138.
239. K. Huo, Y. Li, R. Chen, B. Gao, C. Peng, W. Zhang, L. Hu, X. Zhang and P. K. Chu, *ChemPlusChem*, 2015, **80**, 576-582.
240. S. Yu, X. Peng, G. Cao, M. Zhou, L. Qiao, J. Yao and H. He, *Electrochim. Acta*, 2012, **76**, 512-517.
241. J. Cai, J. Huang, M. Ge, J. Iocozzia, Z. Lin, K. Q. Zhang and Y. Lai, *Small*, 2017, **13**, 1604240.
242. S. Tong, Y. Xu, Z. Zhang and W. Song, *J. Phys. Chem. C*, 2010, **114**, 20925-20931.
243. X. Li, J. Yao, F. Liu, H. He, M. Zhou, N. Mao, P. Xiao and Y. Zhang, *Sens. Actuators B Chem.*, 2013, **181**, 501-508.
244. B. Modrzejewska, A. J. Guwy, R. Dinsdale and D. L. Hawkes, *Water Res.*, 2007, **41**, 260-268.
245. S. Liu and A. Chen, *Langmuir*, 2005, **21**, 8409-8413.
246. A. K. Kafi, G. Wu and A. Chen, *Biosens. Bioelectron.*, 2008, **24**, 566-571.
247. M. Viticoli, A. Curulli, A. Cusma, S. Kaciulis, S. Nunziante, L. Pandolfi, F. Valentini and G. Padeletti, *Mater. Sci. Eng. C*, 2006, **26**, 947-951.
248. S. J. Sadeghi, G. Gilardi and A. E. G. Cass, *Biosens. Bioelectron.*, 1997, **12**, 1191-1198.
249. L. Gorton, A. Lindgren, T. Larsson, F. D. Munteanu, T. Ruzgas and I. Gazaryan, *Anal. Chim. Acta*, 1999, **400**, 91-108.
250. Z. An, Y. Wang and J. He, *J. Mater. Chem.*, 2011, **21**, 15780-15787.
251. M. Liu, G. Zhao, K. Zhao, X. Tong and Y. Tang, *Electrochem. Commun.*, 2009, **11**, 1397-1400.
252. G. Zhao, Y. Lei, Y. Zhang, H. Li and M. Liu, *J. Phys. Chem. C*, 2008, **112**, 14786-14795.
253. Y.-C. Zhu, Q. Wang, L.-B. Zhang, W.-W. Zhao, J.-J. Xu and H.-Y. Chen, *ChemElectroChem*, 2017, **4**, 1011-1015.
254. M. Terracciano, V. Galstyan, I. Rea, M. Casalino, L. De Stefano and G. Sbervegleri, *Appl. Surf. Sci.*, 2017, **419**, 235-

240.
255. S. S. Mandal, K. K. Narayan and A. J. Bhattacharyya, *J. Mater. Chem. B*, 2013, **1**, 3051-3056.
256. Y. An, L. Tang, X. Jiang, H. Chen, M. Yang, L. Jin, S. Zhang, C. Wang and W. Zhang, *Chem. Eur. J.*, 2010, **16**, 14439-14446.
257. P. Kar, A. Pandey, J. J. Greer and K. Shankar, *Lab Chip*, 2012, **12**, 821-828.
258. W. W. Zhao, Z. Liu, S. Shan, W. W. Zhang, J. Wang, Z. Y. Ma, J. J. Xu and H. Y. Chen, *Sci. Rep.*, 2014, **4**, 4426.
259. A. Chaubey, M. Gerard, R. Singhal, V. S. Singh and B. D. Malhotra, *Electrochim. Acta*, 2000, **46**, 723-729.
260. Z. Zhang, R. T. K. Kwok, Y. Yu, B. Z. Tang and K. M. Ng, *ACS Appl. Mater. Interfaces*, 2017, **9**, 38153-38158.
261. J. Zhu, X. Huo, X. Liu and H. Ju, *ACS Appl. Mater. Interfaces*, 2016, **8**, 341-349.
262. M. Kalbacova, J. M. Macak, F. Schmidt-Stein, C. T. Mierke and P. Schmuki, *Phys Status Solidi-R*, 2008, **2**, 194-196.
263. K. Tamura, Y. Ohko, H. Kawamura, H. Yoshikawa, T. Tatsuma, A. Fujishima and J. I. Mizuki, *Electrochim. Acta*, 2007, **52**, 6938-6942.
264. G. Kaur, T. Willsmore, K. Gulati, I. Zinonos, Y. Wang, M. Kurian, S. Hay, D. Losic and A. Evdokiou, *Biomaterials*, 2016, **101**, 176-188.
265. K. Gulati, M. S. Aw and D. Losic, *Int. J. Nanomed.*, 2012, **7**, 2069-2076.

Graphical Abstract:

This review summarizes the recent research progress in the biomedical applications of TNTs. It is demonstrated that TNTs exhibit a unique combination of biocompatibility and surface functionalization ability. TNTs can be used as orthopedic, dental and stent implants with little influence on their shapes and forms. Due to the excellent biocompatibility and controllable size and crystal structure, TNTs structure performs multiple meaningful functions, including regulating cell adhesion, differentiation and proliferation, inducing hydroxyapatite formation, and promoting osseointegration and hemocompatibility. Furthermore, TNTs could be functionalized with biomolecules or therapeutic metal NPs, and loaded with growth factors, antibiotics and anticoagulants. Considerable *in vitro* and *in vivo* studies suggest that TNTs are promising for biomedical applications in future.